UNIVERSIDADE D
COIMBRA

Joana Margarida de Morais Sayal Abreu Campos

Cross-Modal Plasticity in the Auditory Cortex of the Congenitally Deaf

an fMRI study using population receptive field analysis

Dissertação no âmbito do Mestrado Interuniversitário em Neuropsicologia Clínica e Experimental, orientada pelo Professor Doutor Jorge Manuel Castelo Branco de Albuquerque Almeida e pela Doutora Zohar Tal e apresentada à Faculdade de Psicologia e Ciências da Educação da Universidade de Coimbra.

Janeiro de 2022

Faculty of Psychology and Educational Sciences of University of Coimbra

CROSS-MODAL PLASTICITY IN THE AUDITORY CORTEX OF THE CONGENITALLY DEAF

An fMRI study using population receptive field analysis

Joana Margarida de Morais Sayal Abreu Campos

Thesis submitted for the Interuniversity Master in Clinical and Experimental Neuropsychology, supervised by Professor Jorge Almeida and Doctor Zohar Tal and presented to the Faculty of Psychology and Educational Sciences of University of Coimbra.

January 2022

UNIVERSIDADE D
COIMBRA

Resumo

Título: Plasticidade Intermodal no Córtex Auditivo de Surdos Congénitos: Análise de Campos Recetivos Populacionais através de um estudo de IRMf

Palavras-chave: Neuroplasticidade; Imagem por Ressonância Magnética Funcional; Análise de Campos Recetivos Populacionais; Surdez Congénita; Organização Topográfica

A neuroplasticidade é a capacidade manifestada pelo cérebro humano em reorganizar-se e modificar a sua atividade ao longo da vida. Envolve mudanças na estrutura, função, e ligações do cérebro, habitualmente derivadas da exposição a estímulos externos ou internos (como aprender uma nova capacidade), ou como resultado de lesões traumáticas ou privação sensorial. Esta última está presente no caso da perda de visão ou surdez profunda, onde o córtex sensorial privado pode ser recrutado para representar informações sensoriais pertencentes a outras modalidades. Este processo, conhecido como plasticidade intermodal, é o tema central desta tese. Em estudos anteriores, verificou-se que o córtex auditivo de surdos congénitos, mas não de ouvintes, é recrutado durante tarefas visuais. No entanto, não é claro se e até que ponto essas respostas intermodais no córtex auditivo privado representam informações espaciais visuais ou mapeiam o campo visual. Este trabalho aborda essa questão diretamente através de estudos de caso de IRMf, com o objetivo de pesquisar e mapear características de retinotopia no córtex auditivo, similarmente à forma de organização das representações neurais no sistema visual. Dois surdos congénitos e um ouvinte participaram numa experiência de IRMf com estímulos tradicionalmente utilizados para mapear o processamento visual. Foi aplicado um método de retinotopia por ondas progressivas (TWR) e de seguida uma técnica de análise de campos recetivos populacionais (pRF), que tem sido substancialmente usada para mapear gradientes topográficos no cérebro, incluindo retinotopia. Os resultados revelam respostas visuais no córtex auditivo dos surdos congénitos, associadas à apresentação dos estímulos, mas não no participante ouvinte. Estas respostas, predominantemente laterizadas no hemisfério direito, representam o campo visual contralateral e são caracterizadas por grandes campos recetivos, centrados nas proximidades da fóvea. Curiosamente, descobrimos que essas respostas a estímulos visuais refletiam principalmente sinais BOLD negativos no córtex auditivo dos surdos, sugerindo uma representação da informação visual através de sinais de desativação intermodal. Será discutida a interpretação e características dessas representações neuroplásticas e desativações neuronais, assim como os efeitos comportamentais, funcionais e anatómicos da plasticidade intermodal em surdos congénitos.

Summary

Title: Cross-Modal Plasticity in the Auditory Cortex of the Congenitally Deaf: an fMRI study using population receptive field analysis
Keywords: Neuroplasticity; Functional Magnetic Resonance Imaging; Population Receptive Field Analysis; Congenital Deafness; Topographic Organization

Neuroplasticity is the ability of the human brain to reorganize and modify its activity throughout life. It involves changes in the structure, function, and connections within the brain, typically acquired following external or internal stimuli (such as learning a new skill), or as a result of traumatic lesions or sensorial deprivation. The latter is present in the case of profound blindness or deafness, where the sensory-deprived cortex can be recruited to represent sensory information belonging to other modalities. This process, known as cross-modal plasticity, is the core subject of this thesis. Specifically, previous studies indicated that the auditory cortex of congenitally deaf, but not of hearing individuals, is recruited during visual tasks. However, it is not clear if and to what extent these cross-modal responses in the deprived auditory cortex represent visual spatial information or map the visual field. In this work, these questions were addressed directly in an fMRI set of case-studies, aiming to search and map retinotopy features in the auditory cortex, similarly to the well-known organization of neural representations in the visual system. Two congenitally deaf and one hearing participant went through a conventional retinotopy fMRI experiment with visual stimuli designed to map the visual system. We applied both traditional traveling-wave analysis and a biologically inspired population receptive field (pRF) technique, which have been substantially used to map topographic gradients in the brain, including retinotopy. Results reveal retinotopic-related responses in the auditory cortex of the deaf, but not in the hearing, locked to the visual presentation of stimuli. These responses, that were mostly lateralized to the right hemisphere, represented the contralateral visual field and were characterized by large receptive fields, centered to near foveal areas. Interestingly, we found that these responses to visual stimuli predominantly reflected negative BOLD signals in the auditory cortex of the deaf, suggesting that visual information might be represented through cross-modal deactivation signals. The meaning and features of these neuroplastic representations and neuronal deactivations will be discussed, as well the behavioural, functional, and anatomical effects of cross-modal plasticity in the congenitally deaf.

Acknowledgements

Completing this master's and thesis was possible due to the academic and personal contribution of several people during these challenging two and a half years. I would like to express my deepest thanks:

To Dr Zohar Tal, for the time we spent meeting and working together, always with a kind-hearted spirit. For her enthusiasm and encouragement. It has been a pleasure having Dr Zohar as my supervisor, and I have learned so much with her.

To Professor Jorge Almeida, also my supervisor, for making it so interesting to discuss neuroscience, and for always having clear insights and ideas. For always wanting the best possible and pushing me forward. For the opportunity to be part of Proaction Lab for almost 5 years now.

To Professor Óscar Gonçalves, for the support throughout this master on many occasions. And for believing in me.

To Proaction Lab: from post-doctoral researchers, PhD students, research assistants, master's colleagues, and collaborators. I would like to thank their availability, readiness to help, interest in my work, and friendship.

To the team that collected this dataset in Beijing, to the participants, and to Dr Alessio Fracasso, that I unfortunately never met in person, for his expertise in pRF models that was so helpful in our analysis.

To my internship supervisors, Professor Manuela Vilar, Professor Mário Simões and Dr Diana Duro, as my clinical internship overlapped with my thesis for 9 months. I'd like to thank them for their understanding and motivation during this time.

To my friends: in music (OAUC, TAUC, Cithara) and to a very specific group of "always there" friends: Rita, Diana, Mathilde, Simão, Inês and Chico.

To my family, my mother and my father, for being my home and unconditional love and support. To my brother, that is not only close emotionally, but is my partner in music and neuroscience.

Aos meus avós maternos e paternos, para os quais as palavras são difíceis de escolher. Dedico esta tese à minha avó materna e ao meu avô paterno, que partiram em 2021. Sei que ficariam muito felizes e orgulhosos com a conclusão desta etapa.

To Universidade de Coimbra, Universidade de Lisboa and Universidade do Minho. This interuniversity master's experience was very rewarding, even in these pandemic times demanding unprecedented resilience.

This thesis was supported by a Foundation for Science and Technology (FCT) project grant POCI-01-0145-FEDER-030757 | PTDC/PSI-GER/30757/2017 - “SeeingEars - Vendo com os teus ouvidos: como é que a neuroplasticidade devido a surdez congénita interfere com o processamento neuronal e com estratégias de reabilitação auditiva”, and Programa COMPETE.

Table of Contents

1. Introduction....9
1.1. The brain and its topographic organization....9
1.1.1. The visual system and retinotopic organization of V1....9
1.1.2. The auditory system and its tonotopic organization....11
1.2. Neuroplasticity and cross-modal plasticity....13
1.2.1. Deafness in humans: behavioural and neuroimaging findings....14
1.2.1.1. Deafness in humans: behavioural findings....14
1.2.1.2. Deafness in humans: anatomical MRI findings....16
1.2.2. Animal models of deafness....18
1.3. Functional MRI and its use in neuroscience....19
1.4. Techniques for measuring visual field maps....20
1.4.1. Phase encoded retinotopy (travelling wave retinotopy)....21
1.4.2. Population receptive field (pRF) modelling....23
1.4.2.1. pRF analysis: advantages and applications....24
1.5. Current study....25
2. Methods....26
2.1. Participants....26
2.2. Stimuli and procedure....26
2.3. Anatomical and Functional Imaging....28
2.4. fMRI pre-processing....28
2.4.1. Anatomical data pre-processing....28
2.4.2. Functional data pre-processing....28
2.5. Travelling wave retinotopy....29
2.6. Population receptive field modelling....29
3. Results....30
4. Discussion and Conclusion....36
References....41
Annexes....47

List of Figures

Figure 1 Visual Field Maps in V1, V2 and V3 10

Figure 2 Tonotopic Map Layout and Interpretations 12

Figure 3 Visual Field Landmarks 21

Figure 4 Travelling Wave Retinotopy Maps 22

Figure 5 pRF Size Variation With Eccentricity 24

Figure 6 Experimental Stimuli and Procedure 27

Figure 7 Retinotopic Organization of the Visual Cortex in Hearing and Deaf Participants .. 31

Figure 8 Explained Variance in Hearing and Deaf Participants – Medial View 32

Figure 9 Explained Variance in Hearing and Deaf Participants – Lateral View 33

Figure 10 Beta Values (Slope) in Hearing and Deaf Participants 34

Figure 11 Polar Angle, Eccentricity, Horizontal Location and pRF Width in the Deaf 35

Figure A1 TWR Analysis – Phase maps…….. 40

List of Abbreviations

A1	Area A1; Primary Auditory Cortex
AC	Auditory Cortex
BOLD	Blood Oxygen Level Dependent
CIs	Cochlear Implants
DICOM	Digital Imaging and Communications in Medicine
DMN	Default Mode Network
fMRI	Functional Magnetic Resonance Imaging
GLM	General Linear Model
GM	Gray Matter
HG	Heschl's Gyrus
HRF	Hemodynamic Response Function
LGN	Lateral Geniculate Nuclei
LH	Left Hemisphere
MRI	Magnetic Resonance Imaging
NIfTI	Neuroimaging Informatics Technology Initiative
PAC	Primary Auditory Cortex
pRF	Population Receptive Field
RF	Receptive Field
RH	Right Hemisphere
STG	Superior Temporal Gyrus
STS	Superior Temporal Sulcus
TR	Repetition Time
TWR	Travelling Wave Retinotopy
V1	Area V1; Primary Visual Cortex
WM	White Matter

1. Introduction

The human brain has developed and functions in an organized way, creating new connections throughout life, while adjusting to new environments and challenges or when recovering from injury. One major example of this neuroplastic capacity of the brain is the case of congenital sensorial deprivation, such as congenital blindness or deafness. Under these circumstances, the brain reorganizes itself and changes some of its most common functions. Following the findings of Almeida et al. (2015), which showed that the location of visually presented stimuli can be decoded from neural patterns in the auditory cortex of the congenitally deaf, we used functional magnetic resonance imaging (fMRI) and population receptive field (pRF) analysis to investigate whether the auditory cortex (AC) of congenitally deaf subjects represents visual information and whether these representations are organized in a retinotopic format, as it is observed in the visual system. For this analysis, we used as a first approach the technique of travelling wave retinotopy and then population receptive field modelling.

1.1. The brain and its topographic organization

1.1.1. The visual system and retinotopic organization of V1

Vision and the processing of visual information are complex and fundamental abilities that involve both sensation and perception. When light reaches the eye, it travels through the cornea, pupil, lens and hits the retina. Among the several layers of cells that constitute the retina, photoreceptors (rod cells and cone cells) transduce light into neural signals. These neural signals traverse other retinal cells such as the ganglion cells, bipolar cells, and horizontal cells. The output of the ganglion cells proceeds to the cortex via the optic nerves and the blind spot (the point where the axons of the retinal ganglionic cells are joined to create the optic nerves). Decussation happens at the optic chiasm, where half of the fibres from each eye are crossed from one brain hemisphere to another. Most of the optic tract fibres synapse in the lateral geniculate nuclei (LGN), which in turn send their output to the primary visual cortex through the geniculo-striate pathway. This is the most understood pathway, and perhaps the one with larger contribution to human perception, but many other visual routes with specific functions have been discovered. Additional visual pathways include subcortical routes, where the retinal output travels via the superior colliculus and the pulvinar thalamic nucleus, which then send direct projections to extrastriate visual cortex, bypassing the primary visual cortex (V1). This route is important for orientation to stimuli and subsequent eye and body movements (Wurtz et al., 1982). Another visual route to the suprachiasmatic nucleus (SCN) in the hypothalamus

provides information to the biological clock by differentiating between day and night (Klein et al., 1991). Segregation of visual pathways has an evolutionary origin, because for instance sub-cortical pathways are particularly efficient in dealing with unexpected or threatening stimuli that require fast reaction.

Visual cortical neurons have response preferences to particular characteristics of light (e.g., lightness/darkness, changes in brightness or colour, orientation of the stimulus, location in centre or periphery of the visual field) in their receptive field (RF; i.e., the region of space that elicits a response from a given neuron (DeAngelis et al., 1995; Hartline, 1940). Neural responses to visual stimulation are highly organized in the brain – much of the visual cortex is organized into visual field maps (Wandell et al., 2007) that show that neurons whose receptive fields lie next to one another in visual space are located next to one another in the cortex, forming one complete representation of the contralateral visual space (Brewer & Barton, 2012). These are also called retinotopic maps (see example in Figure 1). In fact, the cornea, lens, and photoreceptor sampling mosaic maintain the spatial arrangement of images, allowing them to be preserved in the retina, through an orderly mosaic of the receptive field centres of the ganglion cells. Although this is not completely preserved in the crossing axons of the optic nerve, it is recovered in the axonal projections of the LGN (Wandell & Winawer, 2011). V1 in each hemisphere encodes a hemifield (half of the visual space), with an overrepresentation (i.e., responses over a larger fraction of cortical surface) for stimuli in the central fovea when compared to stimuli shown in the periphery of the visual field (i.e., cortical magnification; Fishman, 1997; Holmes, 1918). V2 and V3 also contain discontinuous hemifield retinotopically organized maps, with borders along the horizontal meridian (Wandell et al., 2007). Borders between visual areas can be drawn while mapping for polar angle preferences (see Figure 1).

Figure 1

Visual Field Maps in V1, V2, and V3

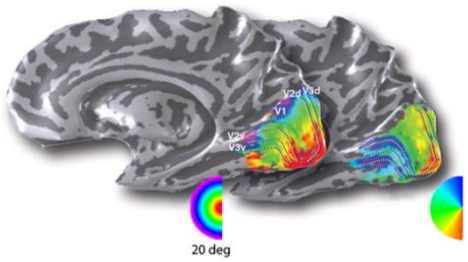

Note. Visual Field Maps in V1, V2, and V3, right hemisphere. These maps were obtained through fMRI using expanding ring and rotating wedge visual stimuli. On the left, the colour

overlay indicates the strongest response for eccentricity (distance to fixation point), and on the right for polar angle. These polar coordinates inform about the location of the receptive field of a given cortical area in V1. From "Visual Field Maps in Human Cortex", by B. Wandell, S. Dumoulin and A. Brewer, 2007, *Cell Press*, 56 (2). Reprinted with permission from Elsevier.

1.1.2. The auditory system and its tonotopic organization

The human auditory system captures changes in air pressure, leading to sound perception. This sensory information is processed and interpreted by the brain, that constructs an internal model of the auditory world based on constancy and past sensory experiences (Ward, 2015). Researchers have shown that auditory processing is highly context-dependent, integrates input from other sensory modalities, depends on experience, and is shaped by cognitive demands such as attention (King et al., 2018). Reflections of the sound waves travel from the outer ear (pinna, auditory canal) through the middle ear (ear drum, malleus, incus, stapes) up to the inner ear (cochlea, semicircular canals). The pressure waves are transduced to neuronal signals by cochlear hair cells, located on the basilar membrane of the cochlea. From the ear to the brain cortex, projections start at the auditory nerve, going to the cochlear nuclei in the brainstem, and then through the medial geniculate nucleus (MGN) ending in the primary auditory cortex (A1), which is located along the Heschl's gyrus (HG) in the temporal lobes. A1 is surrounded by the belt and parabelt regions (Kaas & Hackett, 1999), which are associated with more complex aspects of sound, such as the separation between the "what" and "where" routes (Ward, 2015).

The early auditory system is organized tonotopically, that is the principle that sounds close to each other in frequency are represented by neurons that are spatially close to each other in the brain (Brewer & Barton, 2016; Humphries et al., 2010; Wessinger et al., 1997). There is evidence that neurons located in the central region of the primary auditory cortex (PAC) respond to lower frequencies and outer regions, in the periphery, prefer higher frequencies (Romani et al., 1982). King et al. (2018) define tonotopic representation as the systematic variation in the frequency selectivity of neurons from low to high values. In the case of the auditory system, the receptive field of these sensory neurons relates (most commonly) to their sensitivity to sound frequency (King et al., 2018). Similar to the visual system, the topographic organization starts before the information reaches the cortex: the basilar membrane of the human cochlea in the inner ear responds to tones topographically (frequency selectivity shifted smoothly along the membrane from high to low at each end), an organization that is preserved

throughout the brainstem, medial geniculate nucleus of the thalamus and A1 (Brewer & Barton, 2016).

In comparison to the visual system, there is still some controversy regarding the extent and the large-scale organization of the tonotopic maps within the AC. While it is widely accepted that the PAC contains two mirror-symmetric frequency gradients along the HG, sharing a low-frequency border (da Costa et al., 2011; Formisano et al., 2003; Humphries et al., 2010), their exact orientation in respect to HG is still debated (Saenz & Langers, 2014). Most studies point towards an interpretation that core fields A1 and R fold across the rostral and caudal banks of the HG in a V-shaped gradient orientation, similar to that of non-human primates (Saenz & Langers, 2014) (see Figure 2). Furthermore, tonotopic mapping revealed that tonotopic organization might even persist in areas beyond the auditory core and belt, including areas up to the superior temporal sulcus (STS) (Striem-Amit et al., 2011). However, interpretations of these maps vary. For instance, Talavage et al., (2004) suggest in their fMRI experiments that five areas in the human AC exhibit at least six tonotopic organizations.

Figure 2

Tonotopic Map Layout and Interpretations

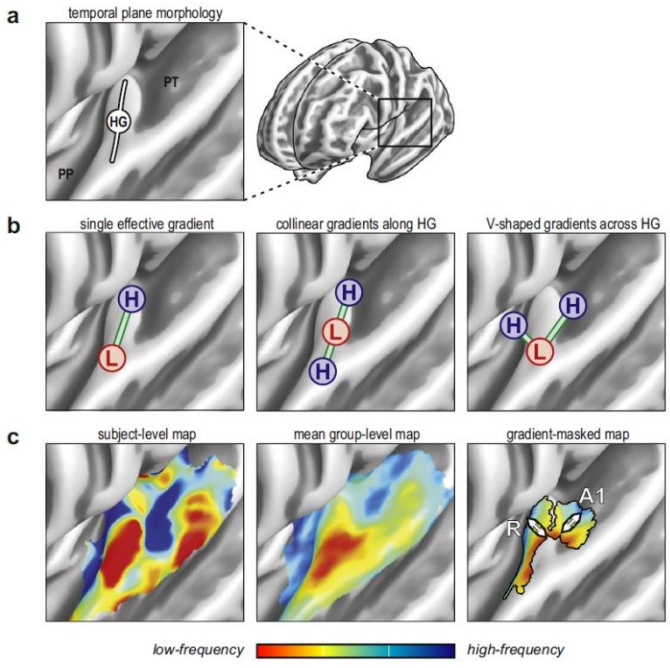

Note. Tonotopic maps in a partially inflated cerebral surface zoomed at the Sylvian fissure **(a)**. Interpretations of the maps regarding the distribution of H (high) and L (low frequencies) **(b)**, and maps on subject level, group-level, and a gradient-masked map **(c)**. A1- primary auditory cortex. HG - Heschl's gyrus; PP - planum polare; PT - planum temporale; R- rostral auditory

area. From "Tonotopic mapping of human auditory cortex", by M. Saenz and D. Langers, 2014, *Hearing Research,* 307:42-52. Reprinted with permission from Elsevier.

Regarding temporal and spatial sensitivity, the auditory system is very well tuned to detect temporal information, while the visual system is superior at processing spatial information (e.g. the auditory system detects rapid changes in frequency, allowing the characterization of sounds such as speech or music, but it is easier to rapidly locate an object in space through vision) (Ward, 2015). Auditory field maps represent spectral (tones) and temporal (period or temporal envelope) aspects of sound (Brewer & Barton, 2016).

1.2. Neuroplasticity and cross-modal plasticity

Individuals with sensory loss are generally able to live independently and accomplish their goals, oftentimes showing impressive performance in their remaining senses. This apparent sensory enhancement might be caused by a phenomenon called cross-modal plasticity: the adaptive reorganization of neurons to integrate the function of a new sensory modality following the loss of another (Frasnelli et al., 2011). This type of neuroplasticity has been mostly studied in animal and human blindness: for instance, people with early blindness become better than sighted controls at judging the direction of pitch change between sounds (Gougoux et al., 2004), or show higher tactile spatial acuity due to Braille reading (Van Boven et al., 2000). Furthermore, morphological differences are also seen in neuroimaging studies. Structures such as the occipital cortex (attributed to vision) have changed dramatically following visual deprivation, being used by non-visual inputs in blind individuals (Collignon et al., 2009).

Our understanding of cross-modal plasticity has also benefited from research on deafness. Animal and human studies have approached the deprived brain, using methods such as functional magnetic resonance imaging (fMRI), electroencephalography (EEG), behavioural responses, and psychophysical tasks to assess differences between control and sensory deprived groups.

Importantly, a proper understanding of the mechanisms of cross-modal plasticity will provide a better insight on the role of sensory input in specifying cortical responses and behaviour. Furthermore, it will also impact the development of better tools to restore sensory modalities for people with sensory loss, as well as better explain success rates of restoration.

1.2.1. Deafness in humans: behavioural and neuroimaging findings

Congenital deafness is the loss of hearing present at birth. This is often attributed to environmental and prenatal factors, such as congenital infections and genetic factors (mutations that affect components of the hearing pathway). It occurs because the ability of the ear to convert the vibratory mechanical energy of sound into the electrical energy of nerve impulses is compromised (Korver et al., 2018).

Several studies have tried to discriminate which functions of the remaining senses are altered in deafness, the cause of these alterations and why these are relevant to behaviour. These findings range from behavioural observations to anatomical and functional MRI findings, related to the enhancement of visual abilities.

1.2.1.1. Deafness in humans: behavioural findings

Deaf individuals have displayed behavioural differences in the way they respond to sensory stimuli: some abilities are similar to those of the hearing, but others seem to be superior. Although this work will focus on the processing of visual information, it has also been demonstrated in other domains such as somatosensation.

Prior to engaging in the specific differences between deaf and hearing groups, an important variable needs to be taken into consideration: the heterogeneity of the deaf population. This is one of the major reasons for variability and dissonance in early deaf studies. Deaf subjects may have different etiologies and genetic markers (e.g., progressive hearing loss vs. profound loss from birth), or language skills. For instance, deaf native signers (proficient in sign language) represent 5% of the deaf population. Nevertheless, being born in a sign language community allows them to develop their language skills at the same time as hearing individuals (Newport et al., 1985). Other deaf humans may have heterogeneous backgrounds, which include subjects with language deprivation, abnormal cognitive development due to communication disruption and comorbidity with other diseases associated with deafness (Mitchell & Karchmer, 2004). Therefore, more recent studies on cross-modal plasticity have been employing more homogeneous groups of the deaf (namely deaf native signers) which reduces some variability and allows for more accurate results, despite the still existing individual differences. Our study and the findings presented below will focus on congenitally deaf participants that are fluent in sign language.

The visual attention of hearing individuals is often engaged by an auditory input (e.g., when an object falls from a shelf, it is most likely the sound of it hitting the floor that will cause a shift of attention and direction of a saccade), an aspect of the auditory system that might be

very important evolutionarily. But how does that work in the deaf? They rely more heavily on their remaining senses, since most of their input from the world comes from the binocular visual field (Frasnelli et al., 2011). This lack of auditory-visual convergence is one of the reasons why Bavelier et al. (2006) proposed that hearing loss leads to changes in higher-level attentional processing, with a redistribution of attentional resources to the peripheral visual field. More recent studies like Bottari et al. (2010) have provided complementary knowledge, stating that these differences arise not only from attentional redistribution, but also reorganized sensory processing.

Differences between deaf and hearing subjects are seen in detecting motion perception changes: deaf participants are superior in detecting small deviations from horizontal movements (Almeida et al., 2018; Hauthal et al., 2013). However, heightened visual abilities as the latter are not widespread in all the areas of visual cognition (Frasnelli et al., 2011). In fact, deaf individuals can show both better and worse visual skills than hearing controls (Bavelier et al., 2006). Basic sensory thresholds such as contrast sensitivity (Finney et al., 2001), motion velocity (Brozinsky & Bavelier, 2004), motion sensitivity (Bosworth & Dobkins, 1999), brightness discrimination (Bross, 1979), and temporal resolution (Nava et al., 2008; Poizner & Tallal, 1987) do not seem to be enhanced in deaf individuals, which is not the case in more complex tasks, where visual attention and processing of the peripheral visual field are manipulated (Almeida et al., 2018). In the absence of auditory input, in order to monitor extrapersonal space, deaf individuals devote greater processing resources to the monitoring of the peripheral visual field (Bavelier et al., 2000) and enhanced neural responses have been reported under conditions of peripheral compared with central attention in congenitally deaf versus hearing controls (Neville & Lawson, 1987). Also, deaf signers appear to be faster at reorienting their attention compared with hearing controls (Parasnis and Samar, 1985). It has been suggested that sign language usage (and consequent analysis of hand motion) might alter motion processing (Bavelier et al., 2001). Bottari et al. (2010) have inclusively shown that the faster reactivity to visual events in the deaf happens regardless of eccentricity – i.e., both centrally and peripherally on the visual field.

In addition to their visual abilities, deaf individuals also appear to outperform controls in tactile sensitivity (Levänen & Hamdorf, 2001), presumably reflecting neuroplasticity and/or attention increase directed to the stimuli (a monotonous sequence of vibratory stimuli). Levänen & Hamdorf (2001) tested for frequency discrimination and detection of random suprathreshold frequency changes, and discovered that congenital deafness enhances the accuracy of suprathreshold tactile change detection.

Overall, but particularly with vision, the stated differences could be easily understood as a compensation for the auditory loss, taking advantage of the auditory-visual convergence typically seen in hearing individuals (but just using vision). The field converges in a common finding: differences in the deaf are focused on abilities that can have a compensatory role regarding early auditory deprivation, such as peripheral visual attention (attention to motion) and orienting mechanisms that have resulted from the reorganization of sensory processing. Deaf individuals show cross modal-plasticity effects particularly on the visual functions that in hearing individuals work in tandem with auditory input. As vision and audition are two important senses needed to navigate through space and time, these compensatory effects can be useful in the perception of daily life danger and spatial orienting. In sum, these behavioural differences are seen mostly in the aspects in which both the deprived and the overtaking sense would provide useful input together (Bell et al., 2019), in order to provide functional advantages. To better understand how these functional and behavioural differences can be represented structurally in the brain, the next section will focus on anatomical studies and how they correlate with functional differences.

1.2.1.2. Deafness in humans: anatomical MRI findings

Morphometric studies of the human brain have attempted to investigate anatomical changes between hearing and deaf individuals. Emmorey et al. (2003), using MRI and volumetric analysis, concluded that deaf and hearing individuals do not differ in gray matter (GM) volume of the HG, but deaf individuals show significantly larger gray matter-white matter ratios than hearing subjects in the HG, having less white matter amount in bilateral HG and other areas of the Superior Temporal Gyrus (STG). However, authors such as Tae (2015) and Amaral et al. (2016) contradict this by showing that the deaf have decreased regional GM volume in the left anterior HG, both inferior colliculi, lingual gyri, nuclei accumbens, and left posterior thalamic reticular nucleus in the midbrain compared to hearing, leading to the hypothesis of an underdevelopment of the AC in the deaf.

Additionally, hemispheric asymmetries have been found in the subcortical visual and auditory brains of the deaf. Amaral et al. (2016) showed that the right thalamus, the right LGN, and the right inferior colliculus are larger than their left counterparts. As the right AC of the deaf has shown neuroplasticity by representing visual information (Almeida et al., 2015; Finney et al., 2001; Nishimura et al., 1999), these asymmetries suggest that the subcortical areas could be rerouting visual information to the AC. There are also studies with diffusion-weighted imaging (Shiell & Zatorre, 2017) and measures of cortical thickness (Shiell et al.,

2016) that correlate the structure of the right planum temporale, a typically auditory region, with visual ability in the deaf. Shiell & Zatorre (2017) found changes in fractional anisotropy, radial diffusivity, and mean diffusivity in the right planum temporale of the deaf, suggesting altered myelination density or crossing fibres. This correlated with the enhanced ability of the deaf to detect visual motion (explored in the next section), evidence of white matter reorganization in favour of visual enhancement. The same region showed increased cortical thickness in the deaf (Shiell et al., 2016).

Overall, these differences suggest that the absence of general auditory perception leads to a less developed AC, particularly when it comes to gray matter in the left hemisphere (LH). However, we observe white matter changes in the right AC, as well as differences in cortical thickness and correlations with functional results, which is consistent with seeing more neuroplastic representations in the right hemisphere (Almeida et al., 2015).

1.2.1.3. Deafness in humans: Functional MRI findings

Multiple functional MRI studies have indicated that people with sensory deprivation exhibit neuroplasticity and recruit their sensory cortices to process information related to their remaining senses. The neuronal reorganization of the brains from people with congenital deafness might lead to the enhancement of visual perception, and is considered a compensatory mechanism, attempting to provide some substitute for the lost modality (Heimler et al., 2014).

Following the findings of behavioural studies, fMRI studies have been showing that the AC of congenitally deaf individuals is recruited for visual tasks. Finney et al. (2001) used a moving dot pattern as the visual stimulus and showed that areas A1 and Brodmann's areas 42 and 22 (auditory association cortex) were processing that stimuli in the right hemisphere. Bola et al. (2017) used temporally complex sequences of stimuli (rhythms) presented in a visual or auditory modality (flashes for visual and beeps for auditory) in deaf and hearing participants, where both groups performed the visual task and the hearing group also performed the auditory equivalent task. Results suggested that the visual task activates the AC (peaking in the posterior lateral part of the high-level AC) in deaf participants, unlike hearing subjects, and that this activation pattern is similar to the one that the hearing group experiences while in the auditory modality of the task. The authors also disclosed increased functional connectivity in the deaf between the AC and dorsal visual cortex (area V5/MT, associated with processing of dynamic visual stimuli), which was not present for the hearing subjects. Along the same line of research, Almeida et al. (2015) implemented an fMRI experiment typically designed to map visual preferences in the visual cortex and showed that the location of a visual stimulus can be

decoded from the patterns of neural activity in the AC of deaf, but not hearing individuals, especially in locations within the horizontal plane and the periphery. Studies with visual motion (Retter et al., 2018) have found stronger direction-selective responses in the STS region in deaf participants and less significantly in the PAC.

As previously mentioned, vision is not the only altered sense in the deaf population. Congenital deafness also affects how the brain processes somatosensation. For instance, the deaf present greater signal change in the rostrolateral HG than hearing individuals while processing somatosensory and bimodal stimuli (double-flash visual illusion induced by two touches to the face) (Karns et al., 2012).

Neuroplasticity might lead to neural reorganization, but it does not necessarily lead to losing its original organizing principles. Literature has shown that despite cross-modal plasticity and sensory deprivation, the AC of the deaf still shows topographic organization: Striem-Amit et al. (2016) used fMRI to look at functional connectivity patterns in the deaf and identified topographic tonotopy-based functional connectivity structures in the AC and extending tonotopic gradients (in auditory core and belt, parabelt, extending to language and speech/voice sensitive regions). This suggests that topographical organization does not need sensory experience to develop and is not affected by brain plasticity.

Overall, fMRI studies have shown that properties such as visual motion (Retter et al., 2018), position in the visual field (Almeida et al., 2015; Finney et al., 2001) and rhythm/frequency discrimination (Bola et al., 2017) are represented in early and/or associative AC of deaf humans due to mechanisms of cross-modal plasticity.

1.2.2. Animal models of deafness

Animal models enable us to examine behaviour without variables or restrains that are attributed to humans (e.g. language). In humans, cross-modal and neuroplastic effects observed in congenitally deaf humans may result from sensory deprivation or from the altered linguistic experience, such as sign language (Bavelier & Neville, 2002). The use of animal models - e.g., cat studies - show us that cortical reorganization happens independently of language acquisition.

Congenitally deaf cats have been considered a suitable model of human congenital deafness (Heid et al., 1998). They show superior performance in visual localization in peripheral visual fields and lower visual movement detection thresholds, compared to hearing cats (Lomber et al., 2010). Lomber and colleagues (2010) used psychophysical tasks and graded cooling, confirming a cross-modal reorganization of the deaf AC. They were able to

localize individual visual processes in portions of the AC, and particularly demonstrate the role of the superficial layers of the dorsal zone of the AC in enhanced visual motion detection in deaf cats. Moreover, in cats, as in humans, cross-modal plasticity is not restricted to vision. Meredith & Lomber (2011) showed that somatosensory and visual modalities participate in cross-modal reinnervation outside A1, in the anterior auditory field of early-deaf cats. Studies in mice using electrophysiological recording techniques combined with cortical myeloarchitecture also showed that the AC of deaf mice contained neurons that responded to somatosensory and visual information, and also that their primary visual area had an increase in size (Hunt et al., 2006).

In sum, animal studies corroborate and share the major findings seen in deaf humans: superiority in localizing stimuli in the peripheral visual field, superiority in motion detection, and neural differences in the processing of both visual and somatosensory information (recruitment of the AC). These findings provide a background for our experiment: the behavioural and functional data clearly show that the AC of the deaf is recruited for visual tasks. More specifically, it processes spatial information regarding the location of visual stimuli. Here, we aim to further explore this cross-modal processing, by investigating if the AC of deaf individuals represents low-level spatial features of visual stimuli, and if these representations are organized in a retinotopic format. We will use fMRI as our neuroimaging method and pRF analysis as our modelling technique. These methods will be described below.

1.3. Functional MRI and its use in neuroscience

Magnetic resonance imaging (MRI) is a technique that uses a strong magnetic field to create images of biological tissue - in our case, the brain. The MR scanner uses a series of changing magnetic gradients and oscillating electromagnetic fields, known as the pulse sequence, causing energy to be absorbed and emitted by the atom's nuclei. Adjustments in parameters of the radio frequency excitation pulses and the magnetic field gradients make it possible to acquire information about structure (anatomical imaging), flow (perfusion imaging), or neural activity (functional imaging) (Logothetis & Wandell, 2004).

In the case of functional MRI (fMRI), it allows for the identification of where in the brain particular mental processes occur, and to characterize those patterns of brain activation. This is possible by measuring changes in blood oxygenation over time, as its levels change rapidly following the activity of neurons in specific brain regions (Huettel et al., 2008). Neural activity leads to the consumption of oxygen, ATP, and glucose, followed by an increase in cerebral blood flow. There is a mismatch between cerebral blood flow and oxygen consumption

(leading to an oversupply of oxygen), which is one of the bases of the blood-oxygen-level-dependent (BOLD) signal. This BOLD signal is sensitive to alterations in deoxygenated haemoglobin levels and cerebral blood volume, and relies on the phenomenon of neurovascular coupling: the link between changes in neuronal activity and the constriction or dilation of micro vessels in the brain (for more on how to interpret the BOLD signal to make inferences about the neural signal see Logothetis & Wandell, 2004).

Besides MRI, several other techniques are used in neuroimaging, such as electroencephalography (EEG), single-unit recording, positron emission tomography (PET), and magnetoencephalography (MEG). All of these differ in their spatial and temporal resolution, how they acquire information, whether their measurements are direct or indirect, and invasiveness. fMRI is a non-invasive technique that has a high spatial resolution, and because of that it is increasingly used in basic and applied neuroscience.

The fMRI BOLD signal that is measured from each voxel (the basic functional unit, usually a 3x3x3 millimetre volumetric unit) represents the average activity of all the neurons within that voxel. Based on the topographic organization of different cortical and subcortical areas, neighbouring cells are characterized by similar receptive fields properties, and thus, their averaged response to stimulation of their receptive field will result in an increase of the BOLD signal. This, as well as the ability of fMRI to obtain signal from the whole brain, make fMRI imaging a useful and efficient method to map the topographic organization of the brain. Today it is one of the most important methods to measure spatial organization, which is what we aim to do. Engel et al. (1994, 1997) used fMRI 27 years ago to measure the retinotopic organization within the human visual cortex, using visual stimuli to map eccentricity and polar angle preferences: specifically, they used expanding rings and rotating wedges respectively. These stimuli were used to create travelling waves of neural activity in the retinotopically organized cortex (see stimuli in Figure 4).

1.4. Techniques for measuring visual field maps

Detailed measurements of visual field maps in individual subjects with fMRI have been performed with several techniques, including the travelling wave retinotopy (TWR) technique and more recently population receptive field (pRF) modelling. TWR - or phase-encoded retinotopy - has been the gold standard paradigm for the last two decades. pRF is an innovative approach that allows for more accurate and complete mapping, and solves some concerns presented by conventional mapping methods.

1.4.1. Phase encoded retinotopy (travelling wave retinotopy)

TWR is a method used in fMRI experiments to measure retinotopic organization in the human cortex and is based on a traveling wave of neural activity within retinotopically organized visual areas, created by the presentation of a visual stimulus. Because of this retinotopic organization, the presentation of stimuli as the rotating wedges and expanding rings (Engel et al., 1994) can elicit a continuous traveling wave of neural activity in the visual cortex (Engel et al., 1997).

The continuous and periodic variation of the visual stimuli location generates fMRI responses that vary systematically in their delay, which is measured as the phase of the sinusoid that best fits the data. While measuring eccentricity preferences (ring expanding from the fovea to periphery), we see that voxels that respond later in time represent more peripheral parts of the visual field, producing a traveling wave of activity moving from the posterior to the anterior part of the calcarine sulcus. This means that the visual field location representations at each voxel are estimated from the relative timing of that voxel's fMRI response. This timing is quantified as the phase of the fMRI signal, calculated by taking the Fourier transform of the voxel's time series (Engel et al., 1994; Engel, 2012).

The two orthogonal dimensions needed to identify a unique location in the visual space (x, y) are polar angle (stimulus is rotating wedge) and eccentricity (stimulus is expanding ring), represented by two polar coordinates: an angle (theta, direction from the centre to the point), and a radius (distance from the centre to the point). Taken together, these two measurements specify the most effective visual field position (Engel et al., 1997; Engel, 2012; Sereno et al., 1995; Wandell et al., 2007) (see Figure 3).

Figure 3

Visual Field Landmarks

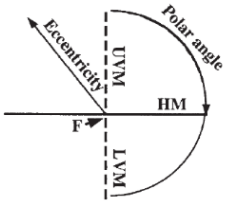

Note. Visual field landmarks and representation of eccentricity (radius) and polar angle (theta) meaning. F – fixation point; HM – horizontal meridian; UVM – upper vertical meridian; LVM – lower vertical meridian. From “Retinotopic Organization in Human Visual Cortex and the

Spatial Precision of Functional MRI", by S. Engel, G. Glover and B. Wandell, 1997, *Cerebral Cortex*, 7(2):181-92. Adapted with permission from Oxford University Press.

These stimuli were designed to maximally stimulate the primary visual cortex and elicit an fMRI signal modulation on the order of 1%-3%, or 15-20 standard deviations above background noise (Brewer & Barton, 2012). An example of retinotopic maps obtained by the TWR method is shown in Figure 4, where we see a selection of voxels that have a powerful response above a defined threshold of coherence, that is the correlation between the response of that voxel and the sinusoidal model, at the frequency of stimulus presentation (Brewer & Barton, 2012).

Figure 4

Travelling Wave Retinotopy Maps – Medial view of the Visual Cortex

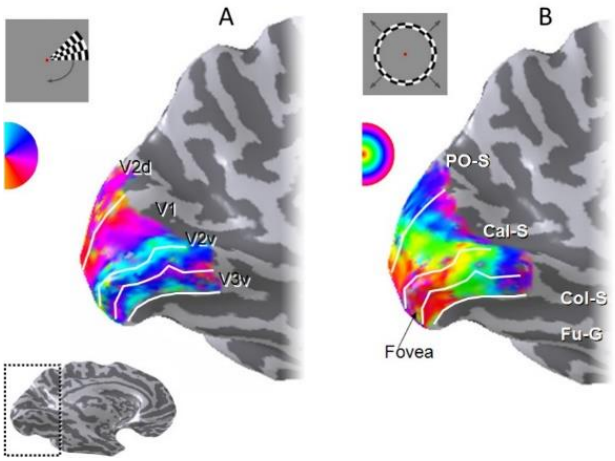

Note. Color map shows the response phase at each location for polar angle **(A)** and eccentricity experiments **(B)**. The solid white lines indicate the boundaries between visual areas. Only voxels with a powerful response at a coherence ≥ 0.25 are coloured. Regarding polar angle preferences, we can see that the lower vertical meridian is represented along the upper bank of the sulcus (A). We also see that foveal preferences fall along the posterior end of the sulcus, and periphery preferences are represented in more anterior locations in the calcarine (B). PO-S, parietal-occipital sulcus; Cal-S, calcarine sulcus. From "Visual Field Map Organization in Human Visual Cortex", by A. Brewer and B. Barton, in *Visual Cortex- Current Status and Perspectives*, 2012, IntechOpen. Reprinted with permission.

These phase-encoded designs using the TWM are informative about neural tuning properties and allow for an estimation of the entire visual field layout, measuring cortical field maps. The application of phase-encoded methods was particularly effective in defining field maps in early visual areas, which are characterized by neurons with small receptive fields that are mostly confined to one hemifield. However, this method is less efficient for mapping areas with large receptive fields that include the fovea (Brewer & Barton, 2012; Wandell et al., 2007). As we are not only analysing early visual areas but also the AC (that might have several receptive field sizes and visual preferences), pRF analysis seemed to be a more advantageous method. Below is a description of this technique and why it is preferable in our study.

1.4.2. Population receptive field (pRF) modelling

pRF modelling is a computational imaging approach that builds models predicting the neural responses to a stimulus, and can be used in a wide range of conditions (in our case, reconstructing cortical visual field maps). It couples fMRI signals (at millimetre scale) with receptive field properties of visual neurons (at micron scale). pRF estimates not only the visual field map, but properties such as receptive field size, laterality, and surround suppression (Dumoulin & Wandell, 2008), and is estimated for individual subjects. These RF properties change systematically across eccentricity and between visual field maps (Fracasso et al., 2016).

The key pRF parameters are receptive field position and receptive field size, units that can be compared over different instruments and different subjects. The shape of the receptive field is a two-dimensional circularly symmetric (isotropic) Gaussian in the visual field, described by field position (x,y) and spread (s), both in visual degrees. For each voxel, the pRF parameters are adjusted to match predicted and measured fMRI time series (Wandell & Winawer, 2015).

pRF analysis can be used in experiments where the traditional mapping stimuli are used, but also with a series of bar patterns that sweep through the visual field in different directions, or a series of stimuli placed at different visual field positions. Figure 5 demonstrates that pRF size increases along the visual hierarchy (from V1 to V3) and, simultaneously, within a given visual area there is a positive correlation between pRF eccentricity and size.

Figure 5

pRF Size Variation With Eccentricity

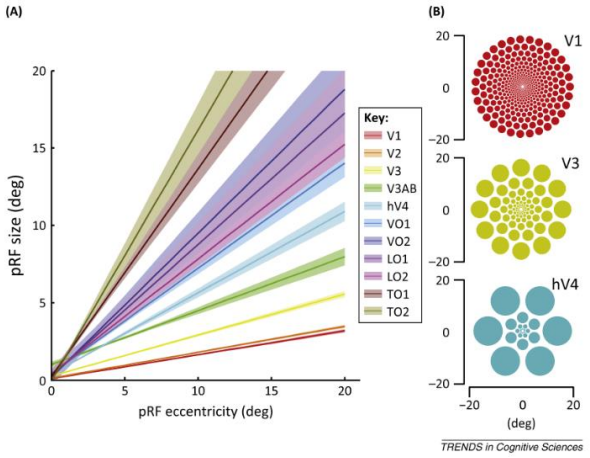

*Note***.** pRF size increases with eccentricity and along the maps in visual areas, with smaller pRF sizes in V1 and larger in ventral and lateral visual areas **(A)**. The increasing radius of each circle, representing pRF size, in each eccentricity position and visual area **(B)**. From "Computational neuroimaging and population receptive fields", by B. Wandell and J. Winawer, 2015, *Trends in Cognitive Sciences*, 19 (6), 349-357. Reprinted with permission from Elsevier.

1.4.2.1. pRF analysis: advantages and applications

Although the pRF method was developed for retinotopic mapping in the visual cortex (Dumoulin & Wandell, 2008), it has had other applications such as measuring tonotopic maps and estimating bandwidth for voxels in the human AC (Thomas et al., 2015). Applications on the study of visual cortical responses using pRF analysis include research on clinical conditions and cognitive task demands (Wandell & Winawer, 2015). Examples are studies on attention (Sprague & Serences, 2013), plasticity of the adult visual cortex (Papanikolaou et al., 2014), developmental plasticity (Haak et al., 2014), psychiatric and neurological disorders such as dementia (Brewer & Barton, 2012) and autism (Hadjikhani et al., 2004; Schwarzkopf et al., 2014).

The advantages of pRF over TWR include the fact that pRF analysis is more precise in the case of visual field maps with large receptive fields. Moreover, pRF analysis provides not only the preferred center for each voxel's pRF but also pRF size/spread. Furthermore, it also provides information on laterality. These are the reasons why pRF was chosen for this study, as it reveals topographical organization more clearly than conventional methods and gives us access to additional information (Brewer & Barton, 2012).

1.5. Current study

In this study, we propose to search for visual responses in the AC of deaf individuals (following up Almeida et al. (2015), Bola et al. (2017) or Finney et al. (2001)) and unravel how these are represented. More specifically, we will search for retinotopy features, such as eccentricity, polar angle, or laterality - features widely documented in the visual cortex (Wandell et al., 2007) - in the AC of two deaf individuals. We will use pRF analysis to determine whether RF size increases with stimulus eccentricity, or whether there are polar angle preferences in the AC of deaf individuals. We will also search for laterality preferences and check for contralateral or ipsilateral representations of the visual field in the AC. Additionally, we are also testing for hemisphere differences in plasticity, since there is past evidence that the right hemisphere (RH) of the deaf shows higher neuroplasticity than the left (Almeida et al., 2015; Finney et al., 2001). Finally, we will also test whether these visual representations are mostly seen in early auditory areas or in the associative AC.

pRF modelling in this dataset was formerly a model considering only positive BOLD signal, therefore a traditional activation model with only positive beta/amplitude values, but then the same model was applied to both increases and decreases of the BOLD signal, including positive and negative beta values. Negative BOLD signal is defined as a drop of the signal below the baseline activity level in a specific brain area, so below the spontaneous activity of a given voxel (Gusnard & Raichle, 2001; Raichle et al., 2001). In our study, we will analyse this signal evoked as a function of the retinal position of a stimulus. Explanations for negative BOLD signal have varied from the purely "vascular blood steal" hypothesis (Harel et al., 2002; Tootell et al., 1998) – where there is a reallocation of cortical blood resources to areas with increased neural activity, resulting in a decrease in cerebral blood flow in the areas with negative BOLD – to a more recent perspective, that is the correlation between negative hemodynamic/BOLD responses and neuronal activity suppression (Shmuel et al., 2006). This standpoint specifies that negative BOLD signal is attributed to decreases in neuronal activity.

Applying pRF modelling on negative BOLD signal might assist enlightening if and to what extent these responses represent topographic information. Negative BOLD has been studied for instance in cross-modal deactivation between sensory cortices (Hairston et al., 2008; Laurienti et al., 2002; Nakata et al., 2019) and pRF analysis has been employed with negative BOLD in studies that explore the Default Mode Network (DMN) (Szinte & Knapen, 2020).

The expression “negative pRF” will be applied to refer to the context where the signal is best predicted by a decrease in BOLD signal below baseline, thence when the negative beta value is the best fit. Detailed methodology is described in the next section.

2. Methods

This experiment aimed to look for visual mapping in the auditory cortex of congenitally deaf participants, using pRF modelling. During the fMRI session, deaf and hearing participants were presented with a full retinotopic experiment, using stimuli typical of visual mapping experiments for early visual cortex (Engel et al., 1994, 1997; Sereno et al., 1995). The patterns of BOLD signal response in the brain were analysed with attention to the visual and auditory cortices. For this experiment, we used part of a dataset collected in Beijing (China) by Almeida et al. (2015), and all the steps from data pre-processing onwards were performed in Coimbra (Portugal).

2.1. Participants

One hearing individual (female, 19 years old) and two congenitally deaf individuals (2 females, 17 and 21 years old) participated in the experiment; all were naive to the purpose of the experiment. All participants had normal or corrected-to-normal vision, no history of neurological disorder, and gave written informed consent in accordance with the guidelines of the institutional review board of Beijing Normal University Imaging Center for Brain Research. Both deaf participants were proficient in Chinese sign language and had hearing loss above 90 dB binaurally (frequencies tested ranged from 125 to 8,000 Hz). One of them never used hearing aids, and the other used a hearing aid on her left ear every day for 10 years since she was 5 years old, which allowed her to perceive sound, but not discriminate between different categories (e.g. voices) or localize its source in space. The causes of deafness in both participants were pregnancy-related complications. The hearing participant reported no hearing impairment or knowledge of Chinese sign language.

2.2. Stimuli and procedure

The stimuli used in the experiment were generated in MATLAB (MathWorks) using the PsychToolbox (Brainard, 1997; Kleiner et al., 2007; Pelli, 1997). Participants were presented with two types of visual stimuli that are typically used to obtain visual field maps: rotating wedges and expanding annuli. The first stimulus was a counterphase flickering (5 Hz) checkerboard wedge (30º) rotating along 12 equidistant positions along the 360º, eliciting

different polar angle preferences (Figure 6A). The second type of stimuli were counterphase flickering (5 Hz) checkerboard annuli expanding in 12 different positions, starting from the central fovea up to the periphery of the visual field, eliciting eccentricity preferences (Figure 6B). Participants were asked to maintain fixation on a central point throughout the entire functional runs. Participants completed twelve runs: six in which the wedge stimuli rotated in clockwise order, starting from the top vertical plane, and six in which the annuli appeared with increasing radius. Each run (with a total of 84 volumes) started with 6 TRs (12 sec) of blank (gray) screen, followed by six repetitions of the full loop of stimuli (72 TRs). TR stands for Repetition Time and is the amount of time between successive pulse sequences applied to the same slice (in our case, 2 seconds). The run finished with a blank screen for 6 TRs. In addition, the MRI session included two runs aimed to estimate the hemodynamic response function (HRF) that were not analysed in this experiment.

Measuring both polar angle and eccentricity is essential for the correct definition of visual field maps, as these two measurements allow for the specific mapping of the responses of the neurons within a single voxel to a unique location in visual space. If we only measured one of these, the cortical response could only be localized to a rather wide range of visual space, which is not sufficient for an accurate delineation of visual field map boundaries (Brewer & Barton, 2012).

Figure 6

Experimental Stimuli and Procedure

A

B

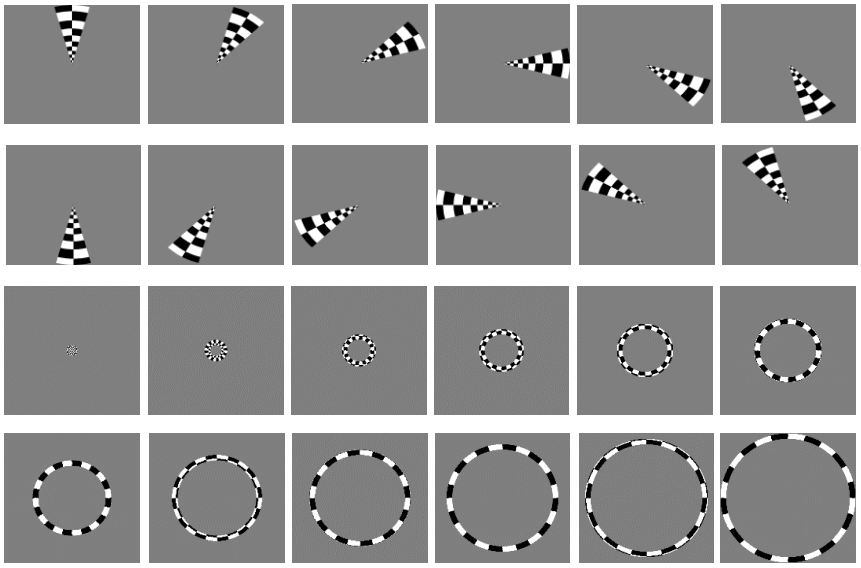

Note. **A: Wedge**. High-contrast, flickering checkerboard that spans the fovea to periphery along twelve specific polar angles (each position lasting 1 TR= 2 sec). This wedge stimulus

rotates clockwise in even positions around a central fixation point, eliciting each voxel's preferred polar angle in the visual space. **B: Ring**. This flickering checkerboard stimulus elicits each voxel's preferred eccentricity by presenting an expanding ring starting from the central fovea up to the periphery, in twelve different positions around a central fixation point (each position lasting 1 TR= 2 sec).

2.3. Anatomical and Functional Imaging

MRI data was collected at the Beijing Normal University MRI center, on a 3 T Siemens Tim Trio scanner. Before running the experiment and acquiring functional data, a high-resolution 3-D structural data set with a 3-D magnetization-prepared rapid-acquisition gradient echo sequence in the sagittal plane was acquired: repetition time (TR) = 2530 ms, echo time (TE) = 3.39 ms, flip angle = 7°, matrix size = 256×256, voxel size = 1×1×1.33 mm, 144 slices, acquisition time = 8.07 min. An echo-planar image sequence was used to collect functional data (TR = 2000 ms, TE = 30 ms, flip angle = 90°, matrix size = 64×64, voxel size = 3.125×3.125×4 mm, 33 slices, interslice distance = 4.6 mm, slice orientation = axial).

2.4. fMRI pre-processing

2.4.1. Anatomical data pre-processing

Processing of the anatomical T1-weighted MR images (white and grey matter segmentation, skull removal, and cortical reconstruction) was performed with Freesurfer (6.0 version) image analysis suite (documented and freely available online (http://surfer.nmr.mgh.harvard.edu/), using the recon-all pipeline.

2.4.2. Functional data pre-processing

The analysis of the functional MRI data was performed in AFNI_21.2.03 (Cox, 1996; Cox & Hyde, 1997), and SUMA (Saad et al., 2004; Saad & Reynolds, 2012) was used for surface-based analysis and visualization.

After converting the data from DICOM to NIfTI files (Li et al., 2016), it went through the typical pre-processing pipeline: slice acquisition time correction, head motion correction, detrending, and deobliquing (EPI dataset transformed to a cardinal orientation; alignment to the AC-PC axis). Functional data was further analysed in subjects' native-space to reduce potential confounds and artefactual effects of normalization procedures (i.e., transforming the participants' functional data to a common brain space such as Talairach or MNI) which is disadvantageous as we are using a pRF approach to look at visual field maps. Working on the

participants' native brain space prevents this loss of information or changes in gradients. Normalization is often performed when group analyses are involved, which is not the case. We did not perform spatial smoothing of the data for the same reason, as it blurs data from adjacent areas within each subject, hampering the processing of differentiating activity coming from adjacent areas (Brewer & Barton, 2012). Following the initial pre-processing steps, the functional data was averaged across runs and volumes, to produce a high-contrast functional volume. This functional volume was used to coregister the functional data to each single subject's anatomic space, using the AFNI functions 3dAllineate and align_epi_anat.py.

2.5. Travelling wave retinotopy

A phase-locking analysis was performed using in-house AFNI code, consisting of the following steps: the functional runs of each stimulus type (rings or wedges) were averaged, to increase the signal-to-noise ratio. A discrete Fourier transform was applied to the averaged time series of each voxel, which extracted the amplitude and the phase of the signal along the frequency domain. These parameters were used to build a pure cosine model, locked to the stimulus repetition frequency (Hertz & Amedi, 2010; Striem-Amit et al., 2011). A Pearson's correlation was calculated between each voxel's time series and the model. The yielded maps include two parameters for each voxel - the correlation coefficient, which served as a measure to the activation level in response to the visual stimulus, and the phase value, which represents the most effective stimulus eccentricity or polar angle that activated a given voxel in the cortex (phase-locked activation). We performed this analysis separately for polar angle (wedge) and eccentricity (ring) representations. The phase of the response is represented by a colour code, overlayed on the anatomical data. For the threshold we used coherence, that is the Pearson's correlation coefficient (r) between the model and the recorded BOLD signal (original time course) at each voxel.

We performed this analysis as a sanity check, to confirm the visual field maps in the visual cortex and search for any neural activation results in the AC.

2.6. Population receptive field modelling

pRF model's scripts and analysis were conducted in R (R Core Team, 2014) and visualization of the models was done through AFNI/SUMA.

First, we generated a set of possible pRF tuning curves based on x and y location (a 28x28 grid of preferred visual locations), range of width (a set of 32 predictors ranging between 0.5 to 11 degrees of the visual field), and a fixed HRF convolution parameter (6-sec peak

latency and 12-sec decay latency). This grid, along with the timing of the stimuli, was used to create a full set of predictors to test. A general linear model (GLM) analysis was applied to each voxel and resulted in a beta value for each one of the predictors. Then, the predictor with the highest beta value was chosen as the best fitted model. For the best model, we can extract information such as x and y position (position on a horizontal and vertical axis with zero on the central fixation point), sigma Pos (width or pRF size; describes the best fitted pRF model and is calculated as the full width at half maximum of the Gaussian), slope (beta value), theta (to infer polar angle), radius (to infer eccentricity) and variance explained (to infer goodness of fit), so how much of the BOLD signal is explained by the model (e.g. a variance explained value of 1 would mean that all BOLD signal activity is attributed and corresponds to the model predictors).

In addition, we calculated a negative pRF model. It followed the same set of pRF tuning curves and GLM procedure, but the best fitted model would be determined by the beta value with the highest absolute value (that could be either positive or negative). A negative beta value results from the negative BOLD signal that is tuned to a specific location in the visual field, leading to a negative slope.

To generate the pRF maps we used the explained variance as the threshold. As in the phase maps resulting from the travelling-wave method we used coherence as *r*, the correlation coefficient, in the case of the pRF maps the explained variance is equivalent to r^2, the coefficient of determination. SUMA (Saad et al., 2004; Saad & Reynolds, 2012) was used as an interactive platform for the visualization of the maps.

3. Results

Individual retinotopic maps were obtained using travelling wave and pRF mapping and were presented on the inflated cortical surface. We started with the phase maps as a sanity check, to confirm the expected visual field maps in the visual cortex (see Figure 1 in Annexes), and search for preliminary results in the auditory cortex. We successfully viewed a retinotopic organization of the visual cortex of our participants (see Annexes), but the representations on the AC were not distinguishable from data noise or other brain areas. Then, we moved forward to our focal analysis technique and generated pRF maps showing the classical results of the retinotopy experiment in the visual cortex in the pRF model with only positive beta values (see Figure 7).

Figure 7

Retinotopic Organization in the Visual Cortex of Hearing and Deaf Participants

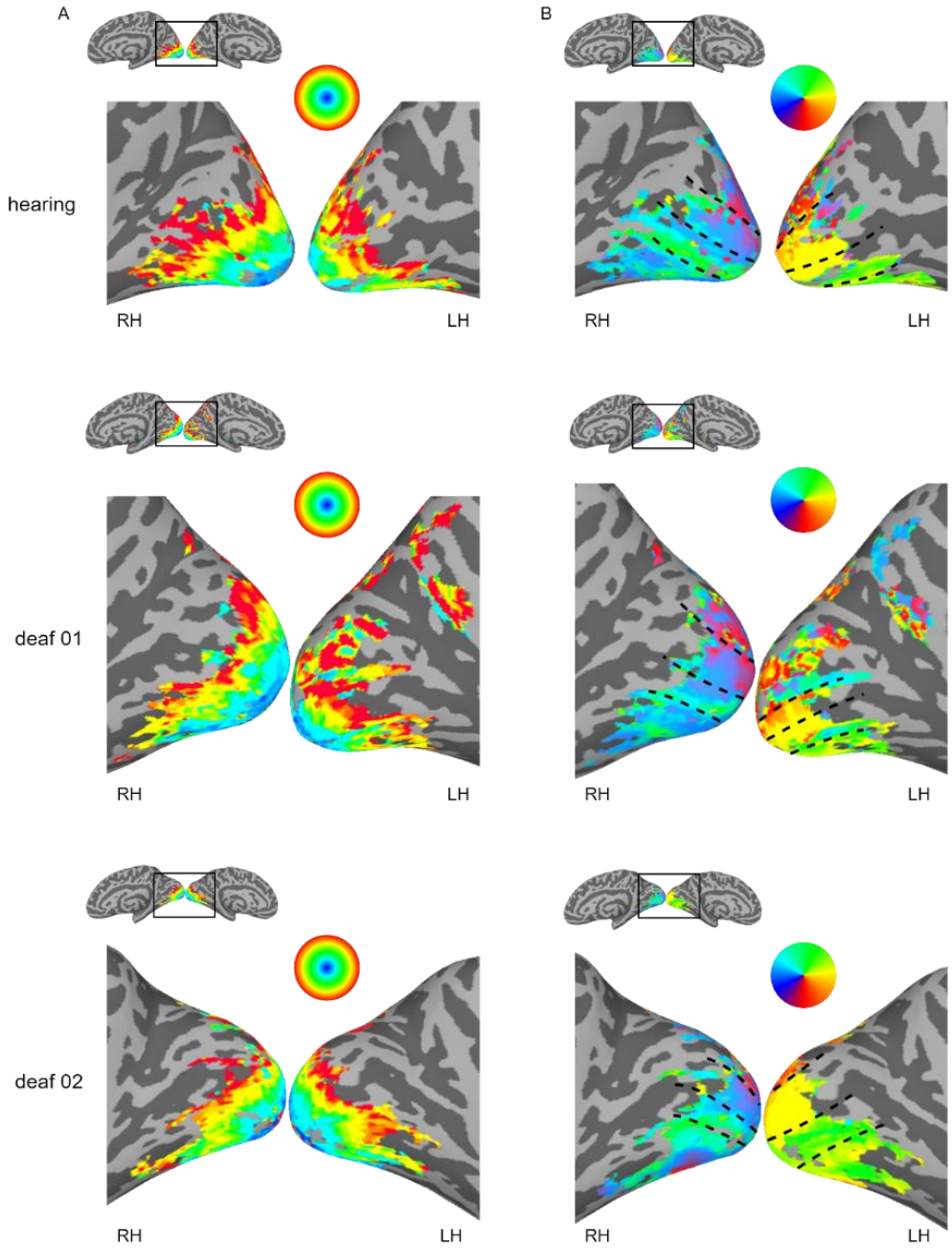

Note. Eccentricity and polar angle representations along the early visual cortex. **A.** eccentricity. The colour blue represents the centre of the visual field (0 visual degrees), up to red (periphery, 6 or more visual degrees) **B.** polar angle (ranging from -π (red) to π). RH- right hemisphere. LH- left hemisphere. Threshold is explained variance ≥ 0.20. Dashed lines delineate the calcarine sulcus and possible borders between V1 and V2. pRF scaled model including only positive beta values.

In this analysis, we expected to see strong visual preferences and organization in early visual areas. We clearly see eccentricity preferences ranging from the fovea to the periphery along the axis of the calcarine sulcus in the early visual cortex. Regarding polar angle, we see a clear contralateral representation of the visual field (RH represents left visual field), and the expected mapping of the stimulus regarding the y/vertical axis. In fact, polar angle is one of the clearer measures to define the borders between V1, V2, and V3. This is particularly discernible for the participants deaf 01 and hearing.

Next, we turned to explore the negative pRF model, by comparing the extracted parameters between the negative and positive models. First, we looked at the variance explained by each one of the models, focusing on early visual areas (see Figure 8). The maps show that both models perform similarly and provide good fitting of the data in the early visual cortex. The negative pRF model covers additional areas compared to the positive model, mainly in medial parietal areas (see Szinte and Knapen (2020) for a similar result). Figure 9 shows the same variance explained maps in a lateral view including the AC.

Figure 8

Variance Explained in Hearing and Deaf Participants – Medial View of the Visual Cortex

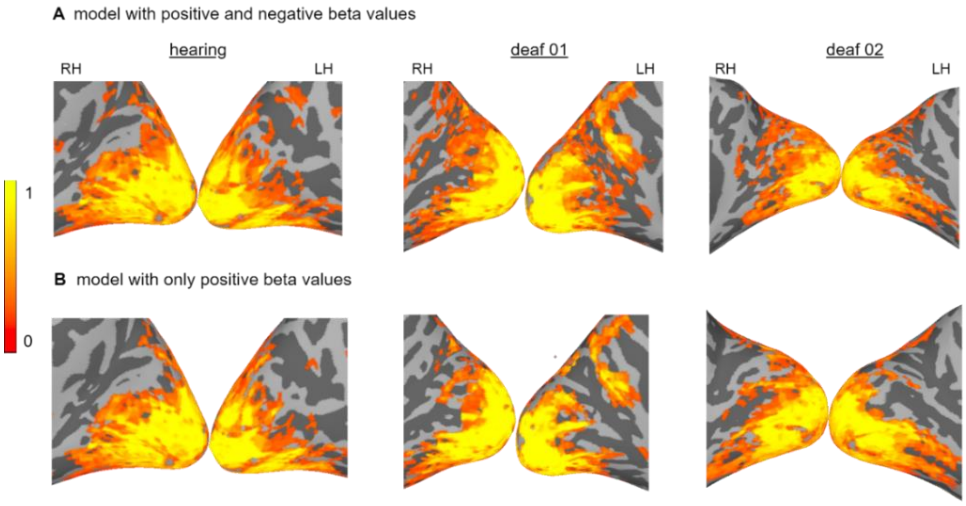

Note. Variance explained in a medial view of early visual areas of the 3 subjects. Threshold is $r^2 \geq 0.08$. pRF scaled model including positive and negative beta values **(A)** and only positive beta values **(B).** RH – right hemisphere; LH- left hemisphere.

Figure 9

Variance Explained in Hearing and Deaf Participants – Lateral view of the Brain

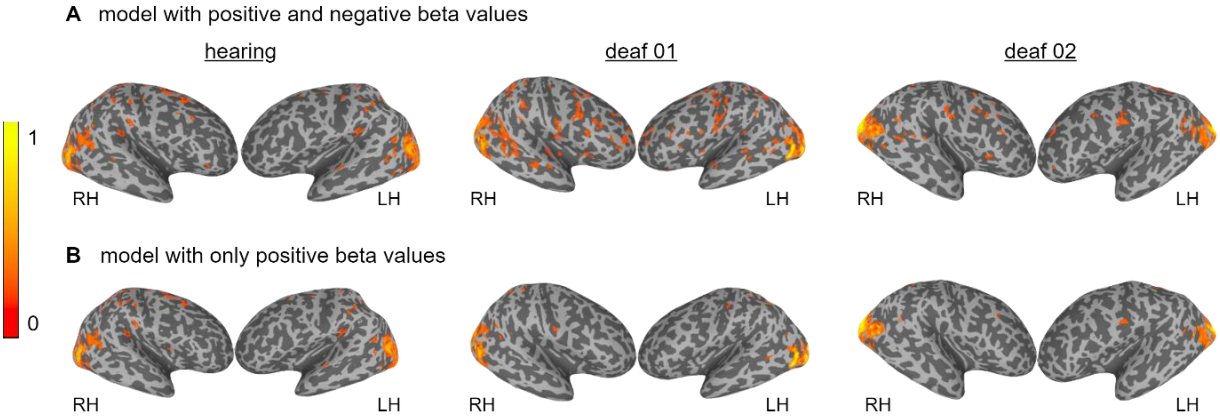

Note. Variance explained in a lateral view of the brain, including the AC. Threshold is $r^2 \geq 0.08$. pRF scaled model including positive and negative beta values **(A)** and only positive beta values **(B)**. The hearing subject does not show differences between models, but the deaf subjects show more clusters of significant explained variance in the model that includes negative beta values (A). RH – right hemisphere; LH- left hemisphere.

Overall, we see that the hearing subject does not appear to show clear differences between the two models, but the deaf show some more variance explained in the model that includes negative beta values. Thus, it seems that potential retinotopic responses in the AC are better captured by the negative pRF model, which led us to focus on the model that includes both positive and negative pRFs in the following analysis steps.

To further characterize the responses to the visual stimuli we plotted the beta values of the best fitted predictor at each cortical location, colour coded by its sign (Figure 10A and 10B). This figure shows that in early visual areas the beta values are predominately positive across the participants, with negative values at the medial parietal cortex (in areas of the DMN, similar to Szinte and Knapen, 2020). On a lateral view (Figure 10A), deaf (but not the hearing) individuals show more representations related to negative betas values, mainly in the prefrontal and temporal lobes. The difference between the hearing and deaf participants is more evident when plotting the negative and positive values in separate maps (Figure 10C and 10D). This is particularly observable in deaf 01, which shows pertinent clusters in the STS, STG, and HG, but also in deaf 02.

Figure 10

Beta Values (Slope) in Deaf and Hearing Participants

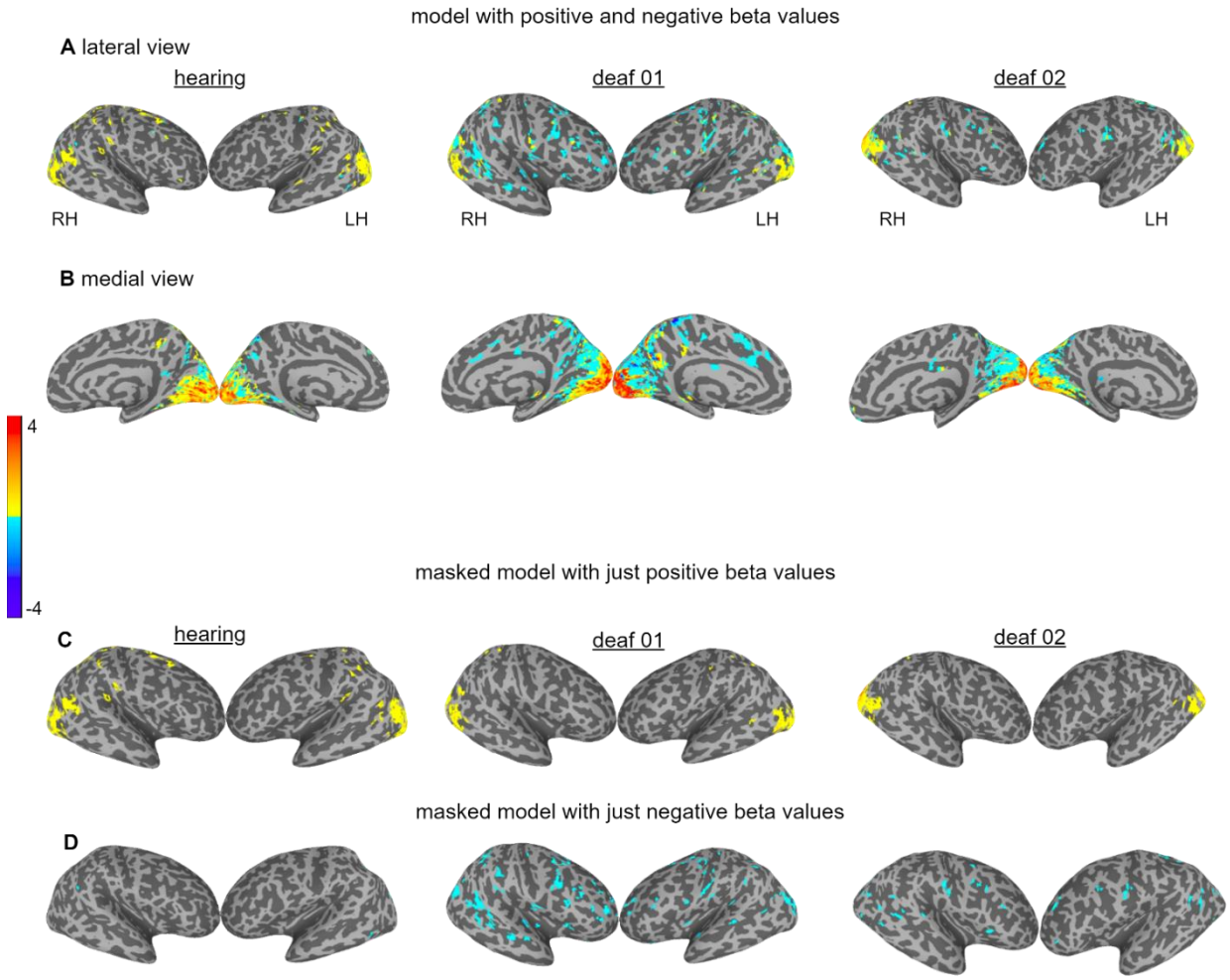

Note. Slope (beta values from ≤ -4 to ≥4, warm colours code positive values and cold colours code negative values), in the lateral **(A)** and medial **(B)** view in the model with positive and negative beta values, and lateral views of the masked model with just positive beta values **(C)** and with just negative beta values **(D)**. Threshold is $r^2 \geq 0.08$.

The findings of Figure 10 lead us to explore which visual features are represented in the auditory areas delineated by the negative model. Since visual responses were seen only in the AC of the deaf and only for negative pRF tuning, we focused on these subjects in the last analysis, aiming to explore which visual features are represented in the AC of the deaf. For that, we extracted the parameters representing polar angle, eccentricity, x location, and pRF size (see Figure 11) only in voxels with negative beta values, as it is the predominant representation in the deaf (but not in the hearing).

Figure 11

Polar Angle, Eccentricity, Horizontal Location and pRF Width in the Deaf

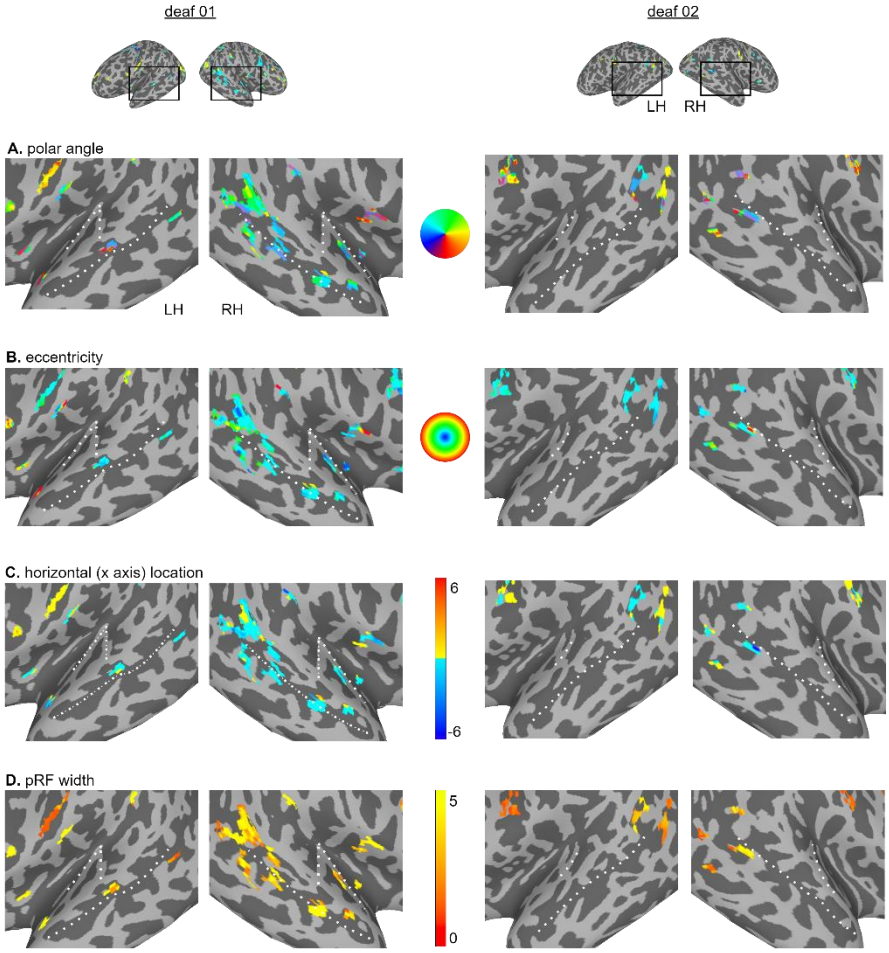

Note. Visual representations in the AC of the deaf participants. These parameters were tested with the masked model with just negative beta values. **A.** Polar angle ranges from -π (red) to π. **B.** In eccentricity preferences, the colour blue represents the centre of the visual field (0 visual degrees), extending until red (periphery, 6 or more visual degrees). **C.** The horizontal visual location was measured on a scale to ≤ -6 to ≥ 6. **D.** pRF size values are between 0 and ≥ 5. Threshold is r^2 ≥0.08. Dotted lines delineate the STS and HG.

We can draw several conclusions regarding these maps: overall, explained variance values are not high in the AC, and although the RH shows stronger responses than the left, there are no clear retinotopic maps. Then, in polar angle, we see representations of the left visual field in the RH, which is contralateral and in accordance with what happens in the visual cortex. The LH does not show clusters large enough to draw any conclusion. Regarding eccentricity, the maps suggest that the preferred area represented in the AC is mostly centre of the visual field, which is not what we expected given the trend towards periphery

representations seen in the literature. X position shows more clearly what we had already seen in polar angle: there is a notable preference for representing the left visual field, particularly in the RH. Width does not seem to show a consistent gradient, but it shows a tendency for high values, meaning a large receptive field size. It also does not seem to be positively correlated with eccentricity preferences.

These clusters in the deaf appear in the RH along the STS, STG, the inferior circular sulcus of the insula and there is also a cluster in the Transverse Temporal Gyrus (TTG), which corresponds to the Heschl's gyrus. This means that they are seen both in early and associative auditory areas, but more significantly in the associative.

4. Discussion and Conclusion

This thesis aimed to investigate cross-modal plasticity in congenitally deaf participants: firstly, by replicating previous results indicating that there are representations of visual information in the AC of the deaf but not the hearing; secondly, by attempting to map these representations, and more specifically, uncover retinotopic features of the AC (if any) that are similar to the visual cortex. This set of single cases included an fMRI experiment with stimuli typically used in classic retinotopic experiments designed to map the visual cortex. We analysed the data with a traditional travelling-wave method, and then focused on our elected technique: the pRF analysis. The results have demonstrated that there are visual-related responses in the AC of the deaf following a cyclic visual presentation, but not in the hearing.

Concerning the retinotopy features, several aspects are of relevance: there are notably more representations in the RH/right AC of the deaf than in the left, and these clusters represent information from the contralateral visual field, therefore corresponding to the left visual field and in accordance with cortical visual processing. This anatomical laterality (predominancy of the RH) in the deaf is coherent with literature on hemispheric asymmetries, where anatomical studies have shown increased white matter volume in the RH compared to the LH (Amaral et al., 2016; Tae, 2015). It also supports fMRI studies stating the supremacy of the right AC of the deaf in representing visual information (Almeida et al., 2015; Finney et al., 2001), finding also present in connectivity and cortical thickness studies: Bola et al. (2017) revealed functional coupling between the AC and area V5 in the deaf (an area responsible for the processing of dynamic visual stimuli), and Shiell et al. (2016) have suggested a behaviour-structure correlation in deaf participants where the ones with better performances at visual motion detection have increased cortical thickness in the right planum temporale.

Regarding the maps representing polar angle and eccentricity, although we do not see clear retinotopic gradients fully covering the visual field, the responses in the AC share some retinotopic features: pRFs in the AC represent information from large parts of the contralateral visual field, and the pRF centres are mostly localized to the foveal or near central part of the visual field. Functional laterality is reinforced by the map of horizontal position, supporting this contralateral representation of the visual field in the RH. pRF size (width) is overall large in the auditory areas but there is no gradient or positive correlation with eccentricity, as it happens with RFs in the visual system (Dumoulin & Wandell, 2008). In fact, if there is a correlation, it tends towards a negative one: we see large width pRFs with centres localized in the fovea, meaning that they represent large parts of the visual field.

Altogether, the values of explained variance are low in the AC of the deaf, compared to the values in the visual system, and deaf 01 clearly shows more clusters in the maps than deaf 02. However, the explained variance values are still higher than the values found in the hearing participant, and higher than the average values obtained at non-visual areas (white matter). Moreover, these clusters appear in anatomical auditory regions that have previously been associated with neuroplasticity following sensorial deprivation: the HG and the STS (Almeida et al., 2015; Daphne Bavelier et al., 2001; Finney et al., 2001; Retter et al., 2018). To give an example, Retter et al. (2018) used visual motion stimuli (random-dot kinematograms) in an fMRI experiment and reported that the PAC of deaf (and not the hearing) shows direction-selective visual motion responses, and that the right STS is extensively recruited for that processing. Bavelier et al. (2001) corroborate this recruitment of the posterior STS in a similar task. These areas belong to the early and associative AC: while the HG is the first cortical structure to process auditory information and is part of the PAC, the STS has been considered the main region for audio-visual integration, although it has also been associated with biological motion perception, speech processing, processing of faces and theory of mind (Hein & Knight, 2008).

A critical finding in our results is that the visual-related responses in the deaf were revealed through the application of the "negative" pRF model - i.e., with the negative beta values. We can discuss the meaning of these negative values, that are associated with negative BOLD signal and therefore would potentially represent neural deactivation or suppression. Negative cross-modal modulation has been reported previously in the literature with hearing population, i.e., visual activity modulating auditory activity in the form of deactivation in the AC (Laurienti et al., 2002; Mozolic et al., 2008). Although some areas of the cortex (poly-sensory areas) can be involved in a variety of higher-order multisensory perceptions, sensory-specific cortices (such as visual and auditory) do not function as independently as it was considered in the past. Laurienti et al. (2002) used fMRI in a passive stimulation paradigm

with 3 conditions (a visual stimulus alone, an auditory stimulus alone, and a combined visual-auditory stimulus) and concluded that visual stimulation resulted in negative BOLD signals in the AC, namely along the superior and middle temporal gyri with a peak in Brodmann area 22 (located in the PAC). A similar effect occurred with the auditory condition, as negative BOLD was observed in voxels of extrastriate visual areas, but not for the combined stimulus condition. Additionally, it has been proposed that the difficulty of the task determines the degree of deactivation (Hairston et al., 2008). This is also true for intra-modal deactivations (Wilson et al., 2019), where negative BOLD responses are elicited within the stimulated cortex, as unilateral stimulus can deactivate the ipsilateral sensory cortex (e.g., unilateral hand movements activate the contralateral sensorimotor cortex and deactivate the ipsilateral cortex (Allison et al., 2000); early visual areas that are tuned to foveal representation respond with positive BOLD signal to foveal visual stimuli and with negative BOLD signal when the stimuli are presented in the periphery, and vice versa (Shmuel et al., 2006).

This task-specific deactivation however is controversial and is not reported in all brain imaging studies using single sensory stimuli (Laurienti et al., 2002). This can be due to different experimental conditions in distinct contexts and with different tasks, and because most studies focus on brain activation and positive modulation results instead of negative BOLD signal and deactivation. We see this contrast in our dataset, among the deaf and hearing participants. Given that all participants were presented with the same stimuli in an equal context, differences between deaf-hearing could arise due to their own functional and anatomical brain properties. It would be erroneous to generalize this hypothesis since a group analysis has not been performed (which would require more participants), but it is an assumption to further explore. Besides, if deactivation/suppressing nonrelevant information contributes to the maximal perceptual integrity and attention to sensory information (Hairston et al., 2008), one could argue that this deactivation is involved in the superior performance of the deaf in some visual tasks, as previously mentioned. They would direct more attention to the task than the hearing participants and therefore exhibit superior abilities. As discussed in the introduction of this thesis, the answer is perhaps found in the middle: enhancements of the congenitally deaf in non-deprived senses result from attention reorienting and neuronal reorganization. Also, we could hypothesize that given that the pRF centres are located near the fovea in the AC of the deaf (and the peak of deactivation happens with foveal representations), this deactivation might sharpen their ability to distinguish between central and peripheral visual representations.

Nevertheless, intra and cross-modal deactivations between sensory cortices are not the only occasions where negative BOLD is present. Various studies regarding the DMN mention deactivation, negative BOLD signal, and inclusively use pRF as an analysis technique. As a matter of fact, Szinte & Knapen (2020) coined the term “negative pRFs” to refer to signals

better predicted by deactivation. They used fMRI and pRF analysis to prove that the DMN selectivity deactivates as a function of the position of a visual stimulus, and that it acts as a negatively modulated high level visual network. This shares some similarity with our results (both in deaf and hearing but mostly in deaf) in medial parietal areas, belonging to the DMN (see figure 10B) - that englobes regions in the lateral prefrontal, posteromedial, inferior parietal cortices, as well as regions in the lateral and medial temporal cortex. They also stated, as we did, that the signal resulting from visual areas (both high and low level) is best explained with positive pRF models, so models predicting a positive amplitude modulation (positive slope). Furthermore, they also perceive that these voxels preferably represent the contralateral visual field (as the AC of our deaf subjects, RH) and their RF sizes increased with eccentricity (retinotopy feature that we could not observe). DMN areas typically show activation during rest (Raichle 2001) and self-related high-level cognitive tasks such as episodic and semantic memory or mind wandering and deactivation during attention-demanding and externally oriented tasks (Alves et al., 2019). For instance, motor movements such as hand and foot movements deactivate the DMN (Nakata et al., 2019).

Another aspect we could reflect on is the matter of controlling attention maintenance, by turning an apparently passive task into an active one. In this experiment, the participants viewed the stimuli on the screen and solely had to fixate on the central fixation point. Other identical experiments have used behavioural tasks such as clicking on a response button to report motion direction changes (see Retter et al., 2018), or monitor the stimuli to report the changes in the end of the block (see Bavelier et al., 2001) or even click on a button when the colour of the fixation dot changed (see Szinte & Knapen, 2020). It remains undisclosed whether adding such tasks that modulate spatial attention would increase attention recruitment or attention maintenance throughout the runs of our dataset, and their effects in the amplitude of the BOLD results, either positive or negative in regard to the baseline. We could hypothesise that a larger attention recruitment would provide clearer results.

Various steps can be performed to further explore how the visual cortex of the deaf use additional resources from the brain, namely the AC. In future research, collecting a larger sample might strengthen the results and potentiate a group analysis, contrasting the hearing and the deaf, and different parameters. Even if the pRF model was applied at an individual level, more participants would permit comparisons and generalizations. This would be particularly informative given that deaf 01 and deaf 02 do not behave exactly the same, and it would allow to potentially reinforce the results of deaf 01. Then, a Region of Interest (ROI) analysis with selected areas in the visual and auditory cortices would provide a more detailed statistical analysis of the data. Additional experiments could include repeating this study with other

sensory modalities, such as searching for negative BOLD in the visual cortex of the blind and looking for tonotopic organization in this recruitment or deactivation.

Research on neuroplasticity is relevant to neuroscience and neuropsychology both for its contribution to basic science, i.e., for the state of the art on the brain's topographical organization and reorganization, but also for applied neurorehabilitation purposes: devices such as cochlear implants (CIs) can be developed to compensate for the sensory loss in the deaf population. These implants convert auditory signals into electric impulses delivered to the acoustic nerve, replacing normal cochlear functions, and require a deep comprehension of the deprived brain's ability to reverse changes. Different areas and functions have their own windows of sensitivity and susceptibility to plasticity. Some mechanisms may be available throughout life (cortico-cortical plasticity), but others are hardly maintained in adults (subcortical plasticity) (Bavelier & Neville, 2002). This raises the question of how cross-modal plasticity will interact with the presence of auditory input. If the AC has reorganized to process vision or touch, will neuroplasticity be detrimental for CIs? Human and animal data suggest that it interferes with the resettlement of the regained auditory inputs (Kral et al., 2006; Kral & Sharma, 2012; Sharma et al., 2014). Thus, it can be hypothesised that cross-modal plasticity is adaptive for sensory deprivation but maladaptive for sensory recovery. Heimler et al. (2014) have suggested a more balanced framework for this impact, stating that cross-modal plasticity might also have maladaptive outcomes in sensory deprivation - being related with impaired functions in the remaining senses, namely temporal tactile processing (Bolognini et al., 2012) - and potential adaptive outcomes in sensory restoration – since functionally selective plasticity might facilitate the recovery of specific cognitive functions (Hassanzadeh, 2012). Sensory rehabilitation programmes should consider multisensory substitutions trainings for the deaf, as they more successfully lead to sensory recovery across the lifespan (Heimler & Amedi, 2020).

This thesis was a set of case-studies that aimed at investigating cross-modal plasticity in the AC of congenitally deaf participants through an fMRI experiment using pRF analysis. Results showed retinotopic-related responses predominantly with negative BOLD signal in the AC of the deaf but not in the hearing. Understanding how the brain is organized and reorganized through neuroplasticity contributes for the state of the art in neuroscience, and for a better and more independent experience of the world by people affected by sensory loss.

References

Allison, J. D., Meador, K. J., Loring, D. W., Figueroa, R. E., & Wright, J. C. (2000). Functional MRI cerebral activation and deactivation during finger movement. *Neurology*, *54*(1), 135–142. https://doi.org/10.1212/wnl.54.1.135

Almeida, J., He, D., Chen, Q., Mahon, B. Z., Zhang, F., Gonçalves, Ó. F., Fang, F., & Bi, Y. (2015). Decoding Visual Location From Neural Patterns in the Auditory Cortex of the Congenitally Deaf. *Psychological Science*, *26*(11), 1771–1782. https://doi.org/10.1177/0956797615598970

Almeida, J., Nunes, G., Marques, J. F., & Amaral, L. (2018). Compensatory plasticity in the congenitally deaf for visual tasks is restricted to the horizontal plane. *Journal of Experimental Psychology: General*, *147*(6), 924–932. https://doi.org/10.1037/xge0000447

Alves, P. N., Foulon, C., Karolis, V., Bzdok, D., Margulies, D. S., Volle, E., & Thiebaut de Schotten, M. (2019). An improved neuroanatomical model of the default-mode network reconciles previous neuroimaging and neuropathological findings. *Communications Biology*, *2*(1), 1–14. https://doi.org/10.1038/s42003-019-0611-3

Amaral, L., Ganho-Ávila, A., Osório, A., Soares, M. J., He, D., Chen, Q., Mahon, B. Z., Gonçalves, O. F., Sampaio, A., Fang, F., Bi, Y., & Almeida, J. (2016). Hemispheric asymmetries in subcortical visual and auditory relay structures in congenital deafness. *European Journal of Neuroscience*, *44*(6), 2334–2339. https://doi.org/10.1111/ejn.13340

Bavelier, D., Tomann, A., Hutton, C., Mitchell, T., Corina, D., Liu, G., & Neville, H. (2000). Visual attention to the periphery is enhanced in congenitally deaf individuals. *The Journal of Neuroscience : The Official Journal of the Society for Neuroscience*, *20*(17). https://doi.org/10.1523/jneurosci.20-17-j0001.2000

Bavelier, D., Brozinsky, C., Tomann, A., Mitchell, T., Neville, H., & Liu, G. (2001). Impact of early deafness and early exposure to sign language on the cerebral organization for motion processing. *Journal of Neuroscience*, *21*(22), 8931–8942. https://doi.org/10.1523/jneurosci.21-22-08931.2001

Bavelier, D., Dye, M. W. G., & Hauser, P. C. (2006). Do deaf individuals see better? *Trends in Cognitive Sciences*, *10*(11), 512–518. https://doi.org/10.1016/j.tics.2006.09.006

Bavelier, D., & Neville, H. J. (2002). Cross-modal plasticity: Where and how? *Nature Reviews Neuroscience*, *3*(6), 443–452. https://doi.org/10.1038/nrn848

Bola, Ł., Zimmermann, M., Mostowski, P., Jednoróg, K., Marchewka, A., Rutkowski, P., & Szwed, M. (2017). Task-specific reorganization of the auditory cortex in deaf humans. *Proceedings of the National Academy of Sciences of the United States of America*, *114*(4), E600–E609. https://doi.org/10.1073/pnas.1609000114

Bolognini, N., Cecchetto, C., Geraci, C., Maravita, A., Pascual-Leone, A., & Papagno, C. (2012). Hearing shapes our perception of time: Temporal discrimination of tactile stimuli in deaf people. *Journal of Cognitive Neuroscience*, *24*(2), 276–286. https://doi.org/10.1162/jocn_a_00135

Bosworth, R. G., & Dobkins, K. R. (1999). Left-hemisphere dominance for motion processing in deaf signers. *Psychological Science*, *10*(3), 256–262. https://doi.org/10.1111/1467-9280.00146

Bottari, D., Nava, E., Ley, P., & Pavani, F. (2010). Enhanced reactivity to visual stimuli in deaf individuals. *Restorative Neurology and Neuroscience*, *28*(2), 167–179. https://doi.org/10.3233/RNN-2010-0502

Brainard, D. H. (1997). The Psychophsycis Toolbox. *Spatial Vision*, *10*(4), 433–436.

Brewer, A. A., & Barton, B. (2012). Effects of healthy aging on human primary visual cortex. *Health*, *04*(09), 695–702. https://doi.org/10.4236/health.2012.429109

Brewer, A. A., & Barton, B. (2016). Maps of the Auditory Cortex. *Annual Review of Neuroscience*, *39*, 385–407. https://doi.org/10.1146/annurev-neuro-070815-014045

Brewer, A., & Barton, B. (2012). Visual Field Map Organization in Human Visual Cortex. In *Visual Cortex - Current Status and Perspectives*. https://doi.org/10.5772/51914

Bross, M. (1979). Residual Sensory Capacities of the Deaf: A Signal Detection Analysis of a Visual Discrimination Task. *Perceptual and Motor Skills*, *48*, 187–194. https://doi.org/10.1002/9781118660584.ese1816

Brozinsky, C. J., & Bavelier, D. (2004). Motion velocity thresholds in deaf signers: Changes in lateralization but not in overall sensitivity. *Cognitive Brain Research*, *21*(1), 1–10. https://doi.org/10.1016/j.cogbrainres.2004.05.002

Collignon, O., Voss, P., Lassonde, M., & Lepore, F. (2009). Cross-modal plasticity for the spatial processing of sounds in visually deprived subjects. *Experimental Brain Research*, *192*(3), 343–358. https://doi.org/10.1007/s00221-008-1553-z

Cox, R. W. (1996). AFNI: Software for analysis and visualization of functional magnetic resonance neuroimages. *Computers and Biomedical Research*, *29*(3), 162–173. https://doi.org/10.1006/cbmr.1996.0014

Cox, R. W., & Hyde, J. S. (1997). Software Tools for Analysis and Visualization of FMRI Data NMR in Biomedicine, in press. *NMR Biomed*, *10*(4–5), 171–178. https://afni.nimh.nih.gov/pub/dist/doc/papers/afni_paper2.pdf

DeAngelis, G. C., Ohzawa, I., & Freeman, R. D. (1995). Receptive-field dynamics in the central visual pathways. *Trends in Neurosciences*, *18*(10), 451–458. https://doi.org/10.1016/0166-2236(95)94496-R

Dumoulin, S. O., & Wandell, B. A. (2008). Population receptive field estimates in human visual cortex. *NeuroImage*, *39*(2), 647–660. https://doi.org/10.1016/j.neuroimage.2007.09.034

Emmorey, K., Allen, J. S., Bruss, J., Schenker, N., & Damasio, H. (2003). A morphometric analysis of auditory brain regions in congenitally deaf adults. *Proceedings of the National Academy of Sciences of the United States of America*, *100*(17), 10049–10054. https://doi.org/10.1073/pnas.1730169100

Engel, S. A. (2012). The development and use of phase-encoded functional MRI designs. *NeuroImage*, *62*(2), 1195–1200. https://doi.org/10.1016/j.neuroimage.2011.09.059

Engel, S., Glover, G. H., & Wandell, B. A. (1997). Retinotopic Organization in Human Visual Cortex and the Spatial Precision of Functional MRI. *Cerebral Cortex*, *7*(2), 181–192.

Engel, S., Rumelhart, D. E., Wandell, B. A., Lee, A. T., Glover, G. H., Chichilnisky, E.-J., & Shadlen, M. N. (1994). fMRI of human visual cortex. *Nature*, *369*(6481), 525.

Finney, E. M., Fine, I., & Dobkins, K. R. (2001). Visual stimuli activate auditory cortex in the deaf. *Nature Neuroscience*, *4*(12), 1171–1173. https://doi.org/10.1038/nn763

Fishman, R. S. (1997). Gordon Holmes, the cortical retina, and the wounds of war. *Documenta Ophthalmologica*, *93*(1–2), 9–28. https://doi.org/10.1007/BF02569044

Fracasso, A., Petridou, N., & Dumoulin, S. O. (2016). Systematic variation of population receptive field properties across cortical depth in human visual cortex. *NeuroImage*, *139*, 427–438. https://doi.org/10.1016/J.NEUROIMAGE.2016.06.048

Frasnelli, J., Collignon, O., Voss, P., & Lepore, F. (2011). Crossmodal plasticity in sensory loss. In *Progress in Brain Research* (1st ed., Vol. 191). Elsevier B.V. https://doi.org/10.1016/B978-0-444-53752-2.00002-3

Gougoux, F., Lepore, F., Lassonde, M., Voss, P., Zatorre, R. J., & Belin, P. (2004). Pitch discrimination in the early blind. *Nature*, *430*(6997). https://doi.org/10.1038/nature02689

Gusnard, D. A., & Raichle, M. E. (2001). Searching for a baseline: Functional imaging and

the resting human brain. *Nature Reviews Neuroscience*, *2*(10), 685–694. https://doi.org/10.1038/35094500

Haak, K. V., Langers, D. R. M., Renken, R., van Dijk, P., Borgstein, J., & Cornelissen, F. W. (2014). Abnormal visual field maps in human cortex: A mini-review and a case report. *Cortex*, *56*, 14–25. https://doi.org/10.1016/J.CORTEX.2012.12.005

Hadjikhani, N., Chabris, C. F., Joseph, R. M., Clark, J., McGrath, L., Aharon, I., Feczko, E., Tager-Flusberg, H., & Harris, G. J. (2004). Early visual cortex organization in autism: An fMRI study. *NeuroReport*, *15*(2), 267–270. https://doi.org/10.1097/00001756-200402090-00011

Hairston, W. D., Hodges, D. A., Casanova, R., Hayasaka, S., Kraft, R., Maldjian, J. A., & Burdette, J. H. (2008). Closing the mind's eye: Deactivation of visual cortex related to auditory task difficulty. *NeuroReport*, *19*(2), 151–154. https://doi.org/10.1097/WNR.0b013e3282f42509

Harel, N., Lee, S.-P., Nagaoka, T., Kim, D.-S., & Kim, S.-G. (2002). *Origin of Negative Blood Oxygenation Level-Dependent fMRI Signals*.

Hartline, H. K. (1940). The Receptive Fields of Optic Nerve Fibers. *American Journal of Physiology*, *130*(4), 690–699.

Hassanzadeh, S. (2012). Outcomes of cochlear implantation in deaf children of deaf parents: Comparative study. *Journal of Laryngology and Otology*, *126*(10), 989–994. https://doi.org/10.1017/S0022215112001909

Hauthal, N., Sandmann, P., Debener, S., & Thome, J. D. (2013). Visual movement perception in deaf and hearing individuals. *Advances in Cognitive Psychology*, *9*(2), 53–61. https://doi.org/10.2478/V10053-008-0131-Z

Heid, S., Hartmann, R., & Klinke, R. (1998). A model for prelingual deafness, the congenitally deaf white cat - Population statistics and degenerative changes. *Hearing Research*, *115*(1–2), 101–112. https://doi.org/10.1016/S0378-5955(97)00182-2

Heimler, B., Weisz, N., & Collignon, O. (2014). Revisiting the adaptive and maladaptive effects of crossmodal plasticity. *Neuroscience*, *283*, 44–63. https://doi.org/10.1016/J.NEUROSCIENCE.2014.08.003

Heimler, B., & Amedi, A. (2020). Are critical periods reversible in the adult brain? Insights on cortical specializations based on sensory deprivation studies. *Neuroscience & Biobehavioral Reviews*, *116*, 494–507. https://doi.org/10.1016/J.NEUBIOREV.2020.06.034

Hein, G., & Knight, R. T. (2008). Superior temporal sulcus - It's my area: Or is it? *Journal of Cognitive Neuroscience*, *20*(12), 2125–2136. https://doi.org/10.1162/jocn.2008.20148

Hertz, U., & Amedi, A. (2010). Disentangling unisensory and multisensory components in audiovisual integration using a novel multifrequency fMRI spectral analysis. *NeuroImage*, *52*(2), 617–632. https://doi.org/10.1016/J.NEUROIMAGE.2010.04.186

Holmes, G. (1918). Disturbances of Vision by Cerebral Lesions. *The British Journal of Opthalmology*.

Huettel, S. A., Song, A. W., & McCarty, G. (2008). *Functional Magnetic Resonance Imaging*.

Humphries, C., Liebenthal, E., & Binder, J. R. (2010). Tonotopic organization of human auditory cortex. *NeuroImage*, *50*(3), 1202–1211. https://doi.org/10.1016/j.neuroimage.2010.01.046

Hunt, D. L., Yamoah, E. N., & Krubitzer, L. (2006). Multisensory plasticity in congenitally deaf mice: How are cortical areas functionally specified? *Neuroscience*, *139*(4), 1507–1524. https://doi.org/10.1016/J.NEUROSCIENCE.2006.01.023

Kaas, J. H., & Hackett, T. A. (1999). "What" and "where" processing in auditory cortex. *Nature Neuroscience*, *2*(12), 1045–1047. https://doi.org/10.1038/15967

Karns, C. M., Dow, M. W., & Neville, H. J. (2012). Altered cross-modal processing in the primary auditory cortex of congenitally deaf adults: A visual-somatosensory fMRI study with a double-flash illusion. *Journal of Neuroscience*, *32*(28), 9626–9638. https://doi.org/10.1523/JNEUROSCI.6488-11.2012

King, A. J., Teki, S., & Willmore, B. D. B. (2018). Recent advances in understanding the auditory cortex. In *F1000Research* (Vol. 7). NLM (Medline). https://doi.org/10.12688/f1000research.15580.1

Klein, D., Moore, R., & Reppert, S. (1991). The Suprachiasmatic Nucleus: The Mind's Clock. In *Oxford University Press*.

Kleiner, M., Brainard, D., Pelli, D., Ingling, A., Murray, R., & Broussard, C. (2007). What's new in Psychtoolbox-3. *Perception*, *36*(14), 1–16.

Korver, A. M. H., Smith, R. J. H., Camp, G. Van, Schleiss, M. R., Bitner-Glindzicz, M. a K., Lustig, L. R., Usami, S.-I., & Boudewyns, A. N. (2018). Congenital hearing loss. *Nat Rev Dis Primers*, *3*(0), 1–37. https://doi.org/10.1038/nrdp.2016.94.Congenital

Kral, A., & Sharma, A. (2012). Developmental neuroplasticity after cochlear implantation. *Trends in Neurosciences*, *35*(2), 111–122. https://doi.org/10.1016/j.tins.2011.09.004

Kral, A., Tillein, J., Heid, S., Klinke, R., & Hartmann, R. (2006). Cochlear implants: cortical plasticity in congenital deprivation. *Progress in Brain Research*, *157*, 283–402. https://doi.org/10.1016/S0079-6123(06)57018-9

Laurienti, P. J., Burdette, J. H., Wallace, M. T., Yen, Y. F., Field, A. S., & Stein, B. E. (2002). Deactivation of sensory-specific cortex by cross-modal stimuli. *Journal of Cognitive Neuroscience*, *14*(3), 420–429. https://doi.org/10.1162/089892902317361930

Levänen, S., & Hamdorf, D. (2001). Feeling vibrations: Enhanced tactile sensitivity in congenitally deaf humans. *Neuroscience Letters*, *301*(1), 75–77. https://doi.org/10.1016/S0304-3940(01)01597-X

Li, X., Morgan, P. S., Ashburner, J., Smith, J., & Rorden, C. (2016). The first step for neuroimaging data analysis: DICOM to NIfTI conversion. *Journal of Neuroscience Methods*, *264*, 47–56. https://doi.org/10.1016/j.jneumeth.2016.03.001

Logothetis, N. K., & Wandell, B. A. (2004). Interpreting the BOLD signal. *Annual Review of Physiology*, *66*, 735–769. https://doi.org/10.1146/annurev.physiol.66.082602.092845

Lomber, S. G., Meredith, M. A., & Kral, A. (2010). Cross-modal plasticity in specific auditory cortices underlies visual compensations in the deaf. *Nature Neuroscience*, *13*(11), 1421–1427. https://doi.org/10.1038/nn.2653

Meredith, M. A., & Lomber, S. G. (2011). Somatosensory and visual crossmodal plasticity in the anterior auditory field of early-deaf cats. *Hearing Research*, *280*(1–2), 38–47. https://doi.org/10.1016/J.HEARES.2011.02.004

Mozolic, J. L., Joyner, D., Hugenschmidt, C. E., Peiffer, A. M., Kraft, R. A., Maldjian, J. A., & Laurienti, P. J. (2008). *Cross-modal deactivations during modality-specific selective attention*. https://doi.org/10.1186/1471-2377-8-35

Nakata, H., Domoto, R., Mizuguchi, N., Sakamoto, K., & Kanosue, K. (2019). Negative BOLD responses during hand and foot movements: An fMRI study. In *PLoS ONE* (Vol. 14, Issue 4). https://doi.org/10.1371/journal.pone.0215736

Nava, E., Bottari, D., Zampini, M., & Pavani, F. (2008). Visual temporal order judgment in profoundly deaf individuals. *Experimental Brain Research*, *190*(2), 179–188. https://doi.org/10.1007/s00221-008-1459-9

Neville, H. J., & Lawson, D. (1987). Attention to central and peripheral visual space in a movement detection task: an event-related potential and behavioral study. II. Congenitally deaf adults. *Brain Research*, *405*(2), 268–283. https://doi.org/10.1016/0006-8993(87)90296-4

Nishimura, H., Hashikawa, K., Doi, K., Iwaki, T., Watanabe, Y., Kusuoka, H., Nishimura, T.,

& Kubo, T. (1999). Sign language “heard” in the auditory cortex. *Nature*, *397*(6715), 116. https://doi.org/10.1038/16376

Papanikolaou, A., Keliris, G. A., Papageorgiou, T. D., Shao, Y., Krapp, E., Papageorgiou, E., Stingl, K., Bruckmann, A., Schiefer, U., Logothetis, N. K., & Smirnakis, S. M. (2014). Population receptive field analysis of the primary visual cortex complements perimetry in patients with homonymous visual field defects. *Proceedings of the National Academy of Sciences of the United States of America*, *111*(16). https://doi.org/10.1073/pnas.1317074111

Pelli, D. G. (1997). The VideoToolbox software for visual psychophysics: Transforming numbers into movies. In *Spatial Vision* (Vol. 10, Issue 4, pp. 437–442). VSP. https://doi.org/10.1163/156856897X00366

Poizner, H., & Tallal, P. (1987). Temporal processing in deaf signers. *Brain and Language*, *30*(1), 52–62. https://doi.org/10.1016/0093-934X(87)90027-7

R Core Team. (2014). *R: A language and environment for statistical computing. R Foundation for Statistical Computing*. http://www.r-project.org/

Raichle, M. E., MacLeod, A. M., Snyder, A. Z., Powers, W. J., Gusnard, D. A., & Shulman, G. L. (2001). A default mode of brain function. *Proceedings of the National Academy of Sciences*, *98*(2), 676–682. https://doi.org/10.1073/PNAS.98.2.676

Retter, T. L., Webster, M. A., & Jiang, F. (2018). Directional visual motion is represented in the auditory and association cortices of early deaf individuals. *Journal of Cognitive Neuroscience*, *31*(8), 1126–1140. https://doi.org/10.1162/jocn_a_01378

Romani, G. L., Williamson, S. J., & Kaufman, L. (1982). Tonotopic organization of human auditory cortex. *SCIENCE*, *216*(3), 1202–1211. https://doi.org/10.1016/j.neuroimage.2010.01.046

Saad, Z. S., & Reynolds, R. C. (2012). SUMA. *NeuroImage*, *62*(2), 768–773. https://doi.org/10.1016/j.neuroimage.2011.09.016.SUMA

Saad, Z. S., Reynolds, R. C., Argall, B., Japee, S., & Cox, R. W. (2004). SUMA: An interface for surface-based intra- and inter-subject analysis with AFNI. *2004 2nd IEEE International Symposium on Biomedical Imaging: Macro to Nano*, *2*, 1510–1513. https://doi.org/10.1109/isbi.2004.1398837

Saenz, M., & Langers, D. R. M. (2014). Tonotopic mapping of human auditory cortex. *Hearing Research*, *307*, 42–52. https://doi.org/10.1016/J.HEARES.2013.07.016

Schwarzkopf, D., Anderson, E. J., de Haas, B., White, S. J., & Rees, G. (2014). Larger extrastriate population receptive fields in autism spectrum disorders. *Journal of Neuroscience*, *34*(7), 2713–2724. https://doi.org/10.1523/JNEUROSCI.4416-13.2014

Sereno, M. I., Dale, A. M., Reppas, J. B., Kwong, K. K., Belliveau, J. W., Brady, T. J., Rosen, B. R., & Tootell, R. B. H. (1995). Borders of multiple visual areas in humans revealed by functional magnetic resonance imaging. *Science*, *268*(5212), 889–893. https://doi.org/10.1126/science.7754376

Sharma, A., Campbell, J., & Cardon, G. (2014). Developmental and cross-modal plasticity in deafness: Evidence from the P1 and N1 event related potentials in cochlear implanted children. *International Journal of Psychophysiology*, *95*(2), 135–144. https://doi.org/10.1016/J.IJPSYCHO.2014.04.007

Shiell, M. M., Champoux, F., & Zatorre, R. J. (2016). The Right Hemisphere Planum Temporale Supports Enhanced Visual Motion Detection Ability in Deaf People: Evidence from Cortical Thickness. *Neural Plasticity*, *2016*. https://doi.org/10.1155/2016/7217630

Shiell, M. M., & Zatorre, R. J. (2017). White matter structure in the right planum temporale region correlates with visual motion detection thresholds in deaf people. *Hearing Research*, *343*, 64–71. https://doi.org/10.1016/J.HEARES.2016.06.011

Shmuel, A., Augath, M., Oeltermann, A., & Logothetis, N. K. (2006). Negative functional MRI response correlates with decreases in neuronal activity in monkey visual area V1. *Nature Neuroscience*, *9*(4), 569–577. https://doi.org/10.1038/nn1675

Sprague, T. C., & Serences, J. T. (2013). Attention modulates spatial priority maps in the human occipital, parietal and frontal cortices. *Nature Neuroscience*, *16*(12), 1879–1887. https://doi.org/10.1038/nn.3574

Striem-Amit, E., Almeida, J., Belledonne, M., Chen, Q., Fang, Y., Han, Z., Caramazza, A., & Bi, Y. (2016). Topographical functional connectivity patterns exist in the congenitally, prelingually deaf. *Scientific Reports*, *6*(July), 1–13. https://doi.org/10.1038/srep29375

Striem-Amit, E., Hertz, U., & Amedi, A. (2011). Extensive cochleotopic mapping of human auditory cortical fields obtained with phase-encoding fMRI. *PLoS ONE*, *6*(3). https://doi.org/10.1371/journal.pone.0017832

Szinte, M., & Knapen, T. (2020). Visual Organization of the Default Network. *Cerebral Cortex*, *30*(6), 3518–3527. https://doi.org/10.1093/cercor/bhz323

Tae, W.-S. (2015). Reduced Gray Matter Volume of Auditory Cortical and Subcortical Areas in Congenitally Deaf Adolescents: A Voxel-Based Morphometric Study. *Investigative Magnetic Resonance Imaging*, *19*(1), 1. https://doi.org/10.13104/imri.2015.19.1.1

Thomas, J. M., Huber, E., Stecker, G. C., Boynton, G. M., Saenz, M., & Fine, I. (2015). Population receptive field estimates of human auditory cortex. *NeuroImage*, *105*(206), 428–439. https://doi.org/10.1016/j.neuroimage.2014.10.060

Tootell, R. B. H., Hadjikhani, N., Hall, E. K., Marrett, S., Vanduffel, W., Vaughan, J. T., & Dale, A. M. (1998). The retinotopy of visual spatial attention. *Neuron*, *21*(6), 1409–1422. https://doi.org/10.1016/S0896-6273(00)80659-5

Van Boven, R. W., Hamilton, R. H., Kauffman, T., Keenan, J. P., & Pascual-Leone, A. (2000). Tactile spatial resolution in blind Braille readers. *American Journal of Ophthalmology*, *130*(4), 542. https://doi.org/10.1016/s0002-9394(00)00743-1

Wandell, B. A., Dumoulin, S. O., & Brewer, A. A. (2007). Visual field maps in human cortex. *Neuron*, *56*(2), 366–383. https://doi.org/10.1016/j.neuron.2007.10.012

Wandell, B. A., & Winawer, J. (2011). Imaging retinotopic maps in the human brain. *Vision Research*, *51*(7), 718–737. https://doi.org/10.1016/J.VISRES.2010.08.004

Wandell, B. A., & Winawer, J. (2015). Computational neuroimaging and population receptive fields. *Trends in Cognitive Sciences*, *19*(6), 349–357. https://doi.org/10.1016/j.tics.2015.03.009

Ward, J. (2015). *The Student's Guide to Cognitive Neuroscience* (Third). Psychology Press.

Wessinger, C. M., Buonocore, M. H., Kussmaul, C. L., & Mangun, G. R. (1997). Tonotopy in human auditory cortex examined with functional magnetic resonance imaging. *Human Brain Mapping*, *5*(1), 18–25. https://doi.org/10.1002/(SICI)1097-0193(1997)5:1<18::AID-HBM3>3.0.CO;2-Q

Wilson, R., Mullinger, K. J., Francis, S. T., & Mayhew, S. D. (2019). The relationship between negative BOLD responses and ERS and ERD of alpha/beta oscillations in visual and motor cortex. *NeuroImage*, *199*, 635–650. https://doi.org/10.1016/J.NEUROIMAGE.2019.06.009

Wurtz, R. H., Goldberg, M. E., & Robinson, D. L. (1982). Brain Mechanisms of Visual Attention. *Scientific American*, *246*(6), 124–135. http://www.jstor.org/stable/24966619

Annexes

Figure A1

TWR analysis – phase maps

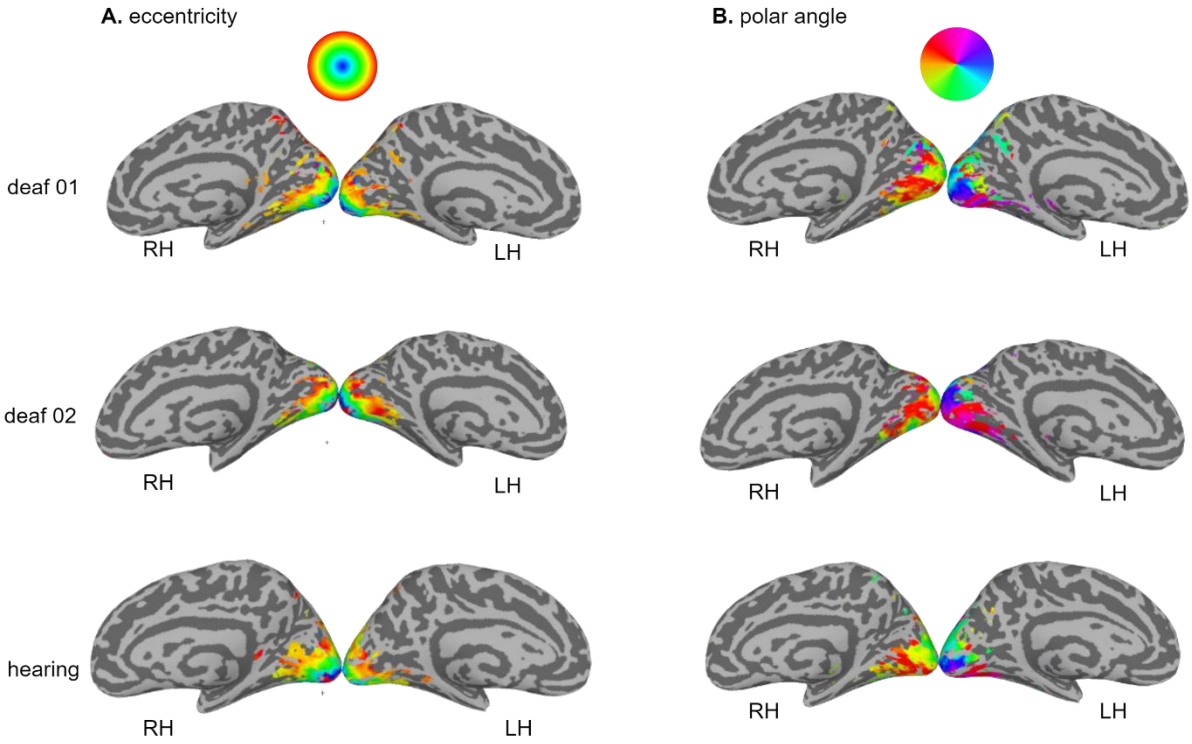

Note. Phase maps. Parameters were the correlation coefficient and the phase value. This analysis was performed separately for (A) eccentricity (ring) and (B) polar angle (wedge) representations. The phase of the response is represented by a colour code, overlayed on the anatomical data. The colour scale in A has blue representing the fovea and red the periphery of the visual filed. The colour scale in B ranges from 0 to 2π. The threshold is coherence ≥ 0.5. RH – right hemisphere. LH – left hemisphere.